



Rui Fiel Cordeiro

Beam-steering Digital num Array Paramétrico

Digital Beam-steering in a Parametric Array



Rui Fiel Cordeiro

Beam-steering Digital num Array Paramétrico

Digital Beam-steering in a Parametric Array

o júri / the jury

presidente / president

Ana Maria Perfeito Tomé

Professora Associada do Departamento de Electrónica, Telecomunicações e Informática da Universidade de Aveiro

vogais / examiners committee

Nuno Miguel da Costa Santos Fonseca

Professor Equiparado a Assistente do 2º. Triénio do Departamento de Engenharia Informática do Instituto Politécnico de Leiria

José Manuel Neto Vieira

Professor Auxiliar do Departamento de Electrónica, Telecomunicações e Informática da Universidade de Aveiro (orientador)

Arnaldo Silva Rodrigues de Oliveira

Professor Auxiliar do Departamento de Electrónica, Telecomunicações e Informática da Universidade de Aveiro (co-orientador)

**agradecimentos /
acknowledgements**

Aproveito para agradecer a todos aqueles que de forma directa ou indirecta me ajudaram na realização deste projecto. Apesar de se tratar dum trabalho individual a contribuição de diversas pessoas foi fundamental para que eu o conseguisse realizar. Em primeiro lugar queria agradecer aos meus orientadores, Professor Doutor José Manuel Neto Vieira e Professor Doutor Arnaldo Silva Rodrigues de Oliveira pela sua disponibilidade e apoio, que foram uma constante ao longo deste projecto. Sem a sua orientação com certeza que o trabalho teria sido muito mais penoso.

Queria de igual modo agradecer à minha família que sempre me incentivou pelo caminho dum melhor formação apoiando-me em todas as etapas. Mais que isso, quero agradecer aos meus pais todo o apoio, carinho e compreensão que demonstraram, especialmente ao longo do projecto realizado. Por fim agradeço também aos elementos das salas 317 e 319, tanto aos seus residentes mais antigos que sempre tiveram a disponibilidade para me mostrarem "os cantos da casa", como aos seus residentes mais recentes pela seu apoio e camaradagem constantes.

Resumo

Actualmente existem diversos métodos que permitem a realização de beam-steering num altifalante paramétrico. No entanto, a maioria dos métodos é incapaz de proporcionar uma elevada resolução angular usando um projecto de hardware eficiente. Mais ainda, poucos são os sistemas que proporcionam um controlo do beam de potência em tempo real.

Neste documento, é proposta uma nova abordagem para colmatar estes problemas tirando partido da alta frequência inerente à modulação sigma-delta. Esta implementação leva a um projecto compacto que proporciona uma elevada resolução angular associada a uma solução de baixo custo e com baixo consumo de potência devido ao uso de apenas uma DAC sigma-delta. O sistema implementado sobre FPGA alia a natural alta frequência dum modulador sigma-delta ao uso dum único shift-register para introduzir os atrasos necessários à realização de beam-steering. A escolha do atraso adequado é feita com o uso de multiplexers que encaminham os diversos sinais sigma-delta para as saídas do sistema desejadas.

Abstract

Several methods enable a steerable beam using an parametric loudspeaker. However, many of them are not able to use a high angular resolution with an efficient design. More, even the ability to change the beam steering in real time is neglected by several methods. In this document, we propose a new approach to the beam-steering problem using the intrinsic high frequency of a sigma-delta digital to analog converter conjugated with on-line configurable digital delays obtained only through a programmable wide shift-register. This implementation leads to a real time beam-steering with a simple digital processing block that enables a high resolution angle. Additionally the use of a sigma-delta DAC provides a low-cost, highly integrated and energy efficient system using only a DAC.

The implemented system takes advantage of the high frequency of the digital signal from the sigma-delta modulator allied with the use of a shift-register to obtain the fine time delays necessary to do the beam-steering. The several outputs delays are chosen between the sigma-delta signals in the shift-register using a group of multiplexers.

Contents

Contents	i
List of Figures	iii
List of Tables	v
List of Acronyms	vii
1 Introduction	1
1.1 Background information	1
1.2 Proposed work and motivation	1
1.3 Objectives	2
1.4 Thesis organization	2
2 Parametric array	5
2.1 Basic concepts and history	5
2.2 Parametric array mechanism	7
2.3 Ultrasound beam modulation	8
2.3.1 Amplitude Modulation - Double Side Band	9
2.3.2 Amplitude Modulation - Single Side Band	10
2.3.3 Phase Modulation	11
2.3.4 Frequency Modulation	12
3 Beam-forming	13
3.1 Introduction	13
3.2 Beam-forming theory	15
3.2.1 One dimension case - linear array	15
3.2.2 Two dimensions case - planar array	17
3.2.3 Power spectrum in space	20
3.2.4 Directivity	21
3.3 Beam-steering	21
3.4 Digital Beam-forming techniques	24
3.4.1 Digital Beam-steering limitations	25
3.4.2 Time domain techniques	27
3.4.3 Frequency domain techniques	27

4	System specifications and simulation	29
4.1	Introduction	29
4.2	System objectives	29
4.3	System delay method	30
4.3.1	Sigma-delta modulator and upsampling	31
4.3.2	1-bit delay network	32
4.3.3	Output stage	32
4.4	Simulation and beam integrity	33
4.4.1	Ideal case	34
4.4.2	Delay quantization	34
4.4.3	Position error	34
5	System design	37
5.1	Introduction	37
5.2	System top level view	37
5.3	ADC	38
5.4	Signal modulation	40
5.5	Beam-former hardware	41
5.5.1	Sigma-Delta DAC	41
5.5.2	Delay Selection	43
5.5.3	Control Unit	44
5.6	Ultrasound transducer array	46
5.6.1	Amplification digital buffers	46
5.6.2	Low pass filters	47
5.6.3	Ultrasound transducers	48
5.7	Hardware simplifications	49
5.8	Hardware resources	50
5.9	Prototypes	51
6	Results	53
6.1	Introduction	53
6.2	Centered beam	54
6.3	Correct position beam-steering test	54
6.4	Angle resolution test	57
6.5	Results commentaries	58
7	Conclusions and future work	61
7.1	Conclusions	61
7.2	Future work	62
A	High order sigma-delta	63
A.1	Introduction	63
A.2	Implemented structure	63
B	Beamformer board	67
	Bibliography	69

List of Figures

2.1	Several ultrasound transducer types.	6
2.2	Example of a SONAR array from a submarine	6
2.3	Comparative scheme of conventional and parametric loudspeaker directivity.	6
2.4	Parametric array produced by Nicera	7
2.5	Double side band amplitude modulator	9
2.6	Single side band amplitude modulator	10
3.1	Example of a beam-forming directional antenna	13
3.2	Example of a loudspeaker array	14
3.3	Beam-forming example	15
3.4	Construction for applying Huyghens' principle.	16
3.5	Linear emitter array simplified	17
3.6	Array patterns	18
3.7	Rectangular array	19
3.8	Used coordinate system.	19
3.9	Example emitter array	20
3.10	Power spectrum density	21
3.11	Steering a wave front	22
3.12	Power spectrum density with beam-steering	24
3.13	Typical beam-steering system	24
3.14	Variation of the smaller steering angle with sampling frequency	26
3.15	Beam-steering system in the time-domain.	27
3.16	Beam-steering system in the frequency-domain.	27
4.1	Ultrasound array pattern	30
4.2	Steering angle depending the sampling frequency	31
4.3	Proposed system block diagram.	31
4.4	First order sigma-delta modulator with 1-bit resolution output.	31
4.5	Delay network.	33
4.6	Beam-forming with exact delays.	34
4.7	Steering angle depending the sampling frequency.	35
4.8	Directivity depending the sampling frequency.	35
4.9	Directivity depending the positioning errors.	36
5.1	GigaBee XC6SLX board and baseboard.	38
5.2	Top level view of the implemented system.	38
5.3	Digilent PmodAD1.	39

5.4	ADC block.	39
5.5	Signal phase modulation block.	40
5.6	DDS core architecture.	41
5.7	PM modulator.	41
5.8	Beam-former hardware.	42
5.9	Sigma-delta modulation.	42
5.10	Implemented sigma-delta modulator.	42
5.11	Delay selection hardware.	44
5.12	Use of multiple beamformers controlled by the same processor.	46
5.13	Output stage and ultrasound transducer array.	46
5.14	TC4469 logic diagram.	47
5.15	Amplification stage	47
5.16	MA40S4S Murata piezoelectric transducer.	48
5.17	Used array pattern.	49
5.18	Sigma-delta modulator output.	49
5.19	Breadboard prototype.	51
5.20	PCB beamformer prototype.	52
6.1	Measuring scheme using a x-y table.	53
6.2	Analysed 40kHz pulse.	54
6.3	Beam direction ($0^\circ, 0^\circ$).	54
6.4	Acoustic pressure results using beam-steering	56
6.5	Acoustic pressure results using beam-steering	58
A.1	Cascade integrator feedback structure.	64
A.2	N-th order sigma-delta modulator.	64
A.3	Basic block internal structure.	65
B.1	Bottom view of the bot part of beamformer board.	67
B.2	Top view of the bot part of beamformer board.	67
B.3	Bottom view of the ultrasound array of beamformer board.	68
B.4	Top view of the ultrasound array part of beamformer board.	68

List of Tables

3.1	Smallest steering angles for common sampling frequencies in sound applications.	26
5.1	FPGA resources used.	50
6.1	Main lobe position test	55
6.2	Angle resolution test.	57

List of Acronyms

ADC	Analog-to-Digital Converter
AM	Amplitude Modulation
A/D	Analog to Digital
CIFB	Cascade Integrator in Feedback
CMOS	Complementary Metal-Oxide Semiconductor
DAC	Digital-to-Analog Converter
DDC	Digital-to-Digital Converter
DDS	Direct Digital Synthesiser
DSB	Double Side Band
DSP	Digital Signal Processor
FIR	Finite Impulse Response
FFT	Fast Fourier Transform
FM	Frequency Modulation
FPGA	Field-Programmable Gate Array
IFFT	Inverse Fast Fourier Transform
IP	Intellectual Property
MSB	Most Significant Bit(s)
MUX	Multiplexer
NCO	Numerically Controlled Oscillator
NTF	Noise Transfer Function
PMOD	Peripheral Module
PM	Phase Modulation
RISC	Reduced instruction set computing

RMS Root Mean Square
SDM Sigma-Delta Modulator
SONAR Sound Navigation and Ranging
SPI Serial Peripheral Interface
SR Shift-Register
SSB Single Side Band
STF Signal Transfer Function
VHDL VHSIC Hardware Description Language

Chapter 1

Introduction

1.1 Background information

Audio applications always were an interesting area in electronics development. The concept, design and improvement of audio related electronics were the nest for many technology developments in areas such as signal processing or signal amplification.

In the last years a new sound reproduction paradigms come up and, between them, the parametric loudspeaker is one of interest. Although discovered around 1960 and commercial applications exist since the mid 1980s, the parametric array only start to be frequently used as an audible loudspeaker in the last years[1][2][3]. This late arrival is mainly due to the advance in transducers technology and signal processing, that now enables cheaper solutions for a better quality in sound reproducing.

For many years, the parametric array, as been used for it's highly directive response in many applications such as the SONAR, medical ultrasonography, seismic prospecting or soil scanning. All of this applications have in common the use of a signal processing technique named beam forming.

Beam forming is the space manipulation of a certain signal and is frequently used to restrict some signals to a limited area in space. The most common reason for this is the analysis of that particular area without interference of signals in other space zones.

In the case of the parametric loudspeaker as an audio application the use of beam forming is rare and the commercial applications that used it are even rarer. Although not very explored, the concept of a controllable directional loudspeaker is already the interest of several academic projects (see [4] and [5]) and is a possible technology with interest for future commercial use.

While common loudspeakers are the best option for filling a room with sound, providing a relatively large space with the same sound conditions they lack the chance for spatial control of that sound. In fact, besides the great progression in technology and digital processing techniques, there are two fundamental areas in sound systems that have been neglected, the control of position and control of distribution[6].

1.2 Proposed work and motivation

The goal of this project is to study, design and create a functional hardware system capable of emitting a very focused steerable audible sound beam. The project is based in several commercial parametric array applications that don't have the beam-steering characteristic.

The addition of a real-time beam-steering capability can bring an increase of the utility of such devices and also the number of applications for them.

Additionally, even the beam-steering being a well explored area in other applications, the proposed method takes a different approach to it trying to achieve a higher angle resolution. It is also of interest the eventual exportation of this concept to other areas such as other ultrasound applications or even radio-frequency systems.

The main work focus on the creation of an effective beam-steering method that can translate in a low cost and efficient implementation. The method simulation, hardware implementation and the system testing are tasks of this project to determine the possibility of its continuation for other projects.

1.3 Objectives

To the realization of this project there were set a group of goal objectives to achieve, divided in main objectives and secondary objectives. Concerning this project the main and fundamental objectives to achieve in the system created are the following:

- Capacity to produce a focused and directional ultrasound beam
- Real-time beam-steering
- Use the primary ultrasound waves in the parametric array to reproduce an audible sound beam

A secondary set of objectives should also be noticed to achieve a better and most efficient implementation:

- The system must be as resource efficient as possible
- The power consumption should be efficient
- It should be possible to create a portable system

1.4 Thesis organization

This document is divided in seven chapters, a brief description of all of them is done in the following paragraphs.

Chapter 1 This chapter presents the motivation to the realized project and the possible applications of it.

Chapter 2 The parametric array phenomena is explained in this chapter as also small introduction to its discovery and analysis history.

Chapter 3 The chapter 3 introduces the beam-forming and beam-steering theory as well as some of the actual digital techniques used to do beam-steering systems.

Chapter 4 The implemented system specifications and used method are described in this chapter. Additionally some system parameters are simulated

Chapter 5 This chapter discusses the hardware used in the project and the design implementation taken.

Chapter 6 It shown and discuss the projected experiments and the results obtained to test the system objectives.

Chapter 7 The last chapter includes the final conclusions and the possible future work.

Chapter 2

Parametric array

2.1 Basic concepts and history

Sound has been used as a communication form by humans and many animals for a long time. Since the beginning that humans tried to invent new ways of sound communication through sound signals, callings or artificially beats.

A sound is a mechanical wave or vibration that can travel through solids, liquids or gases. Depending on the frequency, the sound can be divided into three groups. The infrasounds, for sounds with frequencies up to 20Hz that are inaudible for humans, however audible for some animals. The audible sound is defined between the frequencies that goes from 20Hz to 20kHz. Finally the ultrasounds composed by frequencies higher than 20kHz, also inaudible for humans.

The advance of technology eventually led to the appearance of the first electric loudspeaker. The term loudspeaker can refer to an individual device or driver or a complete system consisting of an enclosure with one or more speakers, their drivers and all the associated electronics.

The first patented electric loudspeaker was created by Alexander Graham Bell as part of his telephone in 1876. The common loudspeaker concept of today, found its first version in 1924 when Chester W. Rice and Edward W. Kellogg introduced the moving-coil principle.

The ultrasound reproduction however, can't be done using a normal loudspeaker. The mechanisms that allow to reproduce signals at ultrasound frequencies are commonly named ultrasonic transducer (some examples are presented in figure 2.1).

An ultrasonic transducer is a device that converts energy into ultrasound, or sound waves above the normal range of human hearing. Commonly these transducers are composed of piezoelectric crystals. These crystals have the property of changing size when a voltage is applied. When an alternate voltage is applied that electric signal will translate in a mechanical vibration, producing sound or ultrasound waves.

An ultrasound array consists in a group of ultrasonic transducers typically disposed in a planar arrangement. This kind of arrays is well known by its very directive response, focusing a relatively small area with almost all the available power. For decades this has been used in several applications such as the SONAR (Sound Navigation And Ranging), medical ultrasonography, seismic prospecting or soil scanning.

The use of an ultrasound array as a mechanism to generate highly directive low frequency (usually audible) beams through higher frequency waves is commonly known as parametric ar-



Figure 2.1: Several ultrasound transducer types.

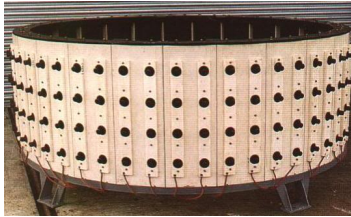


Figure 2.2: Example of a SONAR array from a submarine

ray or parametric loudspeaker. The parametric array was first discovered by Peter Westervelt around the 1950s, but only in 1963 Westervelt was capable of a first theoretical analysis. In his work [7], Westervelt found the link between the emission of two high-frequency collimated beams of sound, commonly referred as primary waves, and the difference signal generated from them. The produced signal derives from a non-linear air demodulation of the primary waves, and its often treated as demodulated signal or wave.

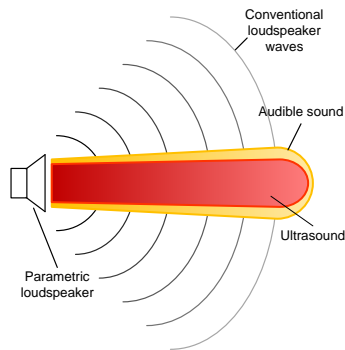


Figure 2.3: Comparative scheme of conventional and parametric loudspeaker directivity.

A few years later, in 1965, Berktaý developed a more accurate and complete description to the parametric array. He introduced his concept of wave "envelope" in his article[8]. The generated signal depends on the envelope function of the primary collimated waves. In fact, according to his theory the scattered sound RMS pressure is proportional to the second time-derivative of the squared envelop of the primary wave. This lead to the possibility of controlling the produced signal by forcing a certain envelope function of the higher frequency waves.

Although the theory was already developed, only in 1975 the parametric array was proved realizable in the air by Bennet and Blacksock[9]. This lead to several exploitations for the

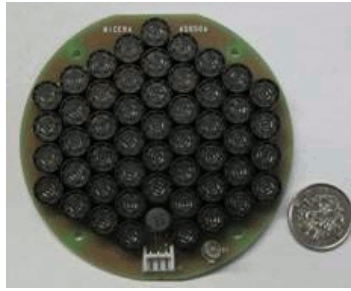


Figure 2.4: Parametric array produced by Nicera

parametric array in audio applications. With the advance in signal processing techniques and the creation of new ultrasonic transducers, several applications tried to improve the audible beam quality and to increase the range of it.

Several methods are used to obtain the audible beam effect combining it with the ultrasonic array high directivity. All of them consist in the same non-linear self-demodulation property of collimated ultrasonic waves. The following section explains the bases for the phenomenon.

2.2 Parametric array mechanism

As Westervelt have discovered, a non-linear interaction between ultrasound waves can be applied with parametric loudspeaker for sound reproduction. Hinged on Berktaÿ's theory, the following analysis similar to the one found in this article[10], explains the relationship between the emitted modulated waves in higher frequencies and the audible sound generated trough the phenomenon of the parametric array.

A emitted pressure wave such as the one emitted by a parametric array can be described the following way,

$$p_1(z, t) = P_0 E(t) e^{-\alpha(t)z} \sin(\omega_0 t + \phi(t)) \quad (2.1)$$

The angular frequency of the wave is defined as ω_0 , and its phase can vary accordingly to the function $\phi(t)$. As for the $e^{-\alpha(t)z}$ is the attenuation constant referred to the thermoviscous attenuation coefficient. P_0 is the initial pressure of of the primary wave and $E(t)$ is its envelope function.

There is some question how might be defined the envelope of a signal wave, since it touches the signal from time to time and might do anything in between. A good and simple definition of it is that the envelope function of a wave defines it's amplitude peaks[11]. In fact the envelope function acts as a amplitude modulation for a higher frequency signal.

According to Berktaÿ's model the pressure of the demodulated wave in air, p_2 , is given by a non-linear phenomenon that can be mathematically described trough the equation 2.2.

$$p_2 \approx \frac{\beta P_0^2 a^2}{16 \rho_0 c_0^4 z} \frac{\partial^2 E^2(t)}{\partial t^2} \frac{1}{\alpha(t)} \quad (2.2)$$

Where β is the coefficient of non-linearity and ρ_0 is the ambient density. The function $\alpha(t)$ is the time varying absorption coefficient and is computed as,

$$\alpha(t) = \left(\omega_0 + \frac{d\phi(t)}{dt} \right)^2 \frac{a_0}{\omega_0^2} = \Omega^2(t) \frac{a_0}{\omega_0^2} \quad (2.3)$$

And the value of $\omega_0 + \frac{d\phi(t)}{dt} = \Omega(t)$ is the instantaneous angular frequency, being $\phi(t)$ the phase function of the wave described in 2.1.

From the equations 2.2 and 2.3 not only the secondary wave is proportional to the second time-derivative squared envelope but also proportional to the inverse second time-derivative of the primary wave instantaneous angular frequency.

$$p_2 \propto \frac{\partial^2}{\partial t^2} \left(\frac{E(t)}{\Omega(t)} \right)^2 \quad (2.4)$$

Manipulating the primary wave envelope function, or instantaneous frequency it is possible to obtain a pretended demodulated signal. The most common way to do it, is using a pre-processing method to modulate a wave with an ultrasound carrier. Several modulations can be applied, as seen in the relation found in 2.4 either amplitude or phase modulations can be used.

2.3 Ultrasound beam modulation

To understand the result of the demodulated signal for each modulation, consider an input signal $x(t)$ at base band and a modulated signal $y(t)$. Consider also that all the modulations use a carrier at the frequency f_c and angular frequency ω_c .

The cases in study can be divided in two groups. The first one are the amplitude modulations. These techniques change only the amplitude of the envelope wave, making the instantaneous angular frequency constant. In this case the relation in 2.4 can be simplified to,

$$p_2 \propto \frac{\partial^2}{\partial t^2} \left(\frac{E(t)}{\Omega_0} \right)^2 \quad (2.5)$$

where Ω_0 is a constant that does not vary with t .

The second group are the phase modulations, that instead of modulating the signal in the envelope wave, do it in the carrier wave phase. In this cases the envelope function is constant with a value of E_0 and the demodulated wave only depends of the function $\Omega(t)$.

$$p_2 \propto \frac{\partial^2}{\partial t^2} \left(\frac{E_0}{\Omega(t)} \right)^2 \quad (2.6)$$

The following subsections of this document will explain four different types of possible modulations to create an audible beam with a parametric array, with both amplitude and phase modulation. There are other methods to do this, however these are the most commonly used and simple to implement. Further more, other pre-processing techniques can be applied together with signal modulations to reduce even more the associated distortion.

2.3.1 Amplitude Modulation - Double Side Band

A common technique used in parametric loudspeakers to modulate the signal is a simple amplitude modulation. Amplitude modulation or AM works by varying the amplitude of the carrier wave accordingly to the source signal and can be described by the equation 2.7.

$$y(t) = [1 + mx(t)]\sin(\omega_c t) \quad (2.7)$$

It is a simple system to implement either in the analog domain as in the digital domain. The amplitude modulator hardware requirements are very simple when comparing with other types of modulations, in fact with only a constant multiplier, a sum and a signal multiplier is possible to create the necessary system to achieve a AM signal.

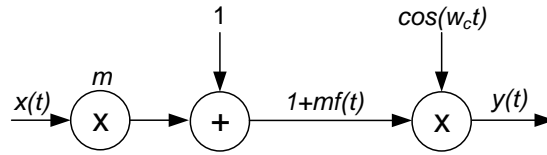


Figure 2.5: Double side band amplitude modulator

Because there is no phase modulation the instantaneous angular frequency $\Omega(t)$ is constant and it's derivative is null. The envelope function is,

$$E_{AM-DSB}(t) = [1 + mx(t)] \quad (2.8)$$

The demodulated wave will be proportional to,

$$\frac{\partial^2}{\partial t^2} E_{AM-DSB}^2(t) = \frac{\partial^2}{\partial t^2} [1 + mx(t)]^2 \quad (2.9)$$

$$\frac{\partial^2}{\partial t^2} E_{AM-DSB}^2(t) = \frac{\partial^2}{\partial t^2} [1 + mx(t) + m^2 x^2(t)] \quad (2.10)$$

$$\frac{\partial^2}{\partial t^2} E_{AM-DSB}^2(t) = \underbrace{mx''(t)}_{\text{signal high pass}} + \underbrace{2m^2[x''(t)x(t) + x'(t)^2]}_{\text{harmonic distortion}} \quad (2.11)$$

The resulting air demodulated signal given by equation 2.18, is a sum of the original signal $x(t)$ second time-derivative plus a signal that is the resulting multiplication of the signal and its time-derivatives. The signal time-derivatives are in fact the signal passed in a high-pass filter which results in a loss of signal at low frequencies.

The factor resulting from the multiplications between the signal and its time-derivatives can be interpreted as harmonic distortion. If the signal were a simple monotonic frequency f_{signal} , the resulting distortion would be a monotonic frequency $f_{distortion} = 2 \times f_{signal}$. However the signal is commonly more complex, a good approximation is a weighted sum of all the frequencies in the signal.

$$x(t) = \sum_{i=1}^N a_i \sin(\omega_i t) \quad (2.12)$$

$$x^2(t) = \left(\sum_{i=1}^N a_i \sin(\omega_i t) \right)^2 \quad (2.13)$$

$$x^2(t) = \sum_{i=1}^N \sum_{j=1}^N a_i a_j (\omega_i + \omega_j)^2 \cos[(\omega_i + \omega_j)t] - \sum_{i=1}^N \sum_{j=1}^N a_i a_j (\omega_i - \omega_j)^2 \cos[(\omega_i - \omega_j)t] \quad (2.14)$$

This means that the harmonic distortion factor creates a mixing in the signal frequencies, in fact the resulting distortion have the sum and difference frequencies of the original signal, which can affect the original signal's frequency band.

2.3.2 Amplitude Modulation - Single Side Band

Another type of AM modulation is the Single-Side Band that eliminates one of the side lobes around the central frequency f_0 in the modulated signal. This modulation is often preferred to the AM-DSB to use with parametric arrays because it produces a lower noise demodulated signal.

It uses an Hilbert transformation to obtain the source signal with a phase delay of exactly 90 degrees. This increases the modulator complexity with the need of one more signal multiplier and the Hilbert transformation block. Commonly this transformation can be achieved in the digital domain with a FIR filter.

Consider that the original signal is $x(t)$ and its Hilbert transformation is $\hat{x}(t)$. The modulated signal can be given by the equation 2.15.

$$y(t) = [1 + mx(t)]\cos(\omega_c t) \mp m\hat{x}(t)\sin(\omega_c t) \quad (2.15)$$

$$y(t) = \cos(\omega_c t) + mx(t)\cos(\omega_c t) \mp m\hat{x}(t)\sin(\omega_c t) \quad (2.16)$$

Where $y(t) = \cos(\omega_c t) + mx(t)\cos(\omega_c t) - m\hat{x}(t)\sin(\omega_c t)$ is the upper band modulation, and $y(t) = \cos(\omega_c t) + mx(t)\cos(\omega_c t) + m\hat{x}(t)\sin(\omega_c t)$ is the lower band modulation.

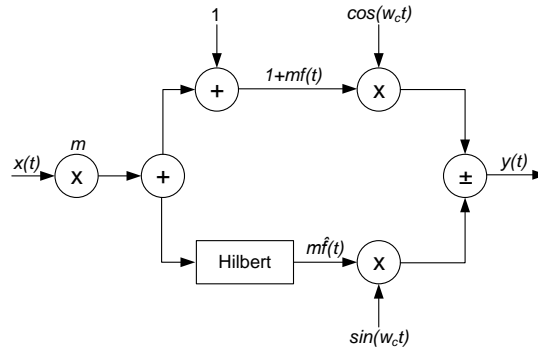


Figure 2.6: Single side band amplitude modulator

The AM-SSB envelope function is given by the equation 2.17

$$E_{AM-SSB}(t) = \sqrt{y^2(t) + \hat{y}^2(t)} \quad (2.17)$$

The demodulated wave in air will be proportional to,

$$\frac{\partial^2}{\partial t^2} E_{AM-SSB}^2(t) = \frac{\partial^2}{\partial t^2} [y^2(t) + \hat{y}^2(t)] \quad (2.18)$$

$$\frac{\partial^2}{\partial t^2} E_{AM-SSB}^2(t) = \frac{\partial^2}{\partial t^2} [1 + m^2(x^2(t) + \hat{x}^2(t)) + 2mx(t)] \quad (2.19)$$

$$\frac{\partial^2}{\partial t^2} E_{AM-SSB}^2(t) = \underbrace{2m^2[x''(t)x(t) + x'^2(t) + \hat{x}''(t)\hat{x}(t) + \hat{x}'^2(t)]}_{\text{harmonic distortion}} + \underbrace{2mx''(t)}_{\text{signal high pass}} \quad (2.20)$$

The resulting signal have an harmonic distortion component and the signal's second time-derivative. When comparing with the AM-DSB for the same signal and same modulation factor m the signals gain is double. Another advantage is that the resulting distortion in the frequency domain has only one side band depending whether the modulation is upper side band or lower side band.

2.3.3 Phase Modulation

Although the use of amplitude modulation to make an audible sound-beam is more commonly used and studied, accordingly to the equation 2.4 the demodulated wave is also proportional to the variation of its phase. Not as empirically perceptible as the resulting demodulation due to the envelope function, it can have lower noise and harmonic distortion.

Consider now that the wave envelope is constant and therefore its second time-derivative is null. Also, the phase modulation with frequency f_c is given by the equation 2.21.

$$y(t) = \sin(\omega_c t + mx(t)) \quad (2.21)$$

Where $x(t)$ is the signal to modulate and m is the modulation index varying in the interval $[0, 2\pi]$. The instantaneous angular frequency is,

$$\Omega(t) = \frac{d}{dt} [\omega_c t + mx(t)] \quad (2.22)$$

$$\Omega(t) = \omega_c + mx'(t) \quad (2.23)$$

The demodulated wave will be proportional to,

$$\frac{\partial^2}{\partial t^2} \frac{1}{\Omega_{PM}(t)} = \frac{\partial^2}{\partial t^2} \left(\frac{1}{\Omega(t)} \right) \quad (2.24)$$

$$\frac{\partial^2}{\partial t^2} \frac{1}{\Omega_{PM}(t)} = 2 \left(\frac{3\Omega^2(t)}{\Omega^4(t)} - \frac{\Omega''(t)}{\Omega^3(t)} \right) \quad (2.25)$$

From the equation 2.24 and switching the function $\Omega(t)$ we have,

$$\frac{\partial^2}{\partial t^2} \frac{1}{\Omega_{PM}(t)} = \frac{6m^2 x''^2(t)}{(\omega_c + mx'(t))^4} - \frac{2mx'''(t)}{(\omega_c + mx'(t))^3} \quad (2.26)$$

In ultrasound applications where the carrier frequencies are above 20kHz it is fair to admit that $\omega_c \gg m$. The equation 2.26 can be simplified to,

$$\frac{\partial^2}{\partial t^2} \frac{1}{\Omega_{PM}(t)} \approx \underbrace{\frac{6m^2 x''^2(t)}{\omega_c^4}}_{\text{harmonic distortion}} - \underbrace{\frac{2mx'''(t)}{\omega_c^3}}_{\text{signal high pass}} \quad (2.27)$$

When comparing with the distortion, the signal has an higher gain, in fact the gain of the signal is $\frac{\omega_c}{3m}$ times bigger that the distortion. Considering that the carrier frequency in ultrasound is bigger than 20kHz this difference is big enough to ignore the harmonic distortion generated by the non-linear air demodulation.

2.3.4 Frequency Modulation

$$y(t) = \sin(\omega_c t + m \int_0^t x(t) dt) \quad (2.28)$$

Where $x(t)$ is the signal to be modulated and m the modulation index varying in the interval $[0, 2\pi]$. The instantaneous angular frequency is given by the equation

$$\Omega(t) = \frac{d}{dt} [\omega_c t + m \int_0^t x(t) dt] \quad (2.29)$$

If $X(t)$ is such a function that $\frac{d}{dt} X(t) = x(t)$, then $\Omega(t)$ is,

$$\Omega(t) = \frac{d}{dt} [\omega_c t + m(X(t) - X(0))] \quad (2.30)$$

$$\Omega(t) = \omega_c + mx(t) \quad (2.31)$$

From equation 2.24 it is possible to extrapolate the following result

$$\frac{\partial^2}{\partial t^2} \frac{1}{\Omega_{FM}(t)} = 2 \left(\frac{3\Omega'^2(t)}{\Omega^4(t)} - \frac{\Omega''(t)}{\Omega^3(t)} \right) \quad (2.32)$$

$$\frac{\partial^2}{\partial t^2} \frac{1}{\Omega_{FM}(t)} = \frac{6m^2 x'^2(t)}{(\omega_c + mx(t))^4} - \frac{2mx''(t)}{(\omega_c + mx(t))^3} \quad (2.33)$$

Once again the value of ω_c is much bigger that m , and the equation 2.32 can be simplified to,

$$\frac{\partial^2}{\partial t^2} \frac{1}{\alpha_{PM}(t)} \approx \underbrace{\frac{6m^2 x'^2(t)}{\omega_c^4}}_{\text{harmonic distortion}} - \underbrace{\frac{2mx''(t)}{\omega_c^3}}_{\text{signal high pass}} \quad (2.34)$$

The result of the air demodulation in a parametric array with FM is very similar to the one obtain with PM, in fact the only difference is in the high band pass order.

Chapter 3

Beam-forming

3.1 Introduction

Beam-forming or beam-steering refer to the set of techniques that allow to manipulate the radiation pattern of several wave emitters, this is, the process of forming beams towards the desired direction while simultaneously suppressing signals originating from other directions. When arranged in patterns in a line, array or solids arrangements, each individual element creates an interference with the remaining signals, this interference can be whether constructive or destructive, and can help to achieve an higher gain to a certain spatial area comparing to an omnidirectional emitter[12].

The term beam-forming can also be used when the spatial filtering of a sensor array is done. This is often used to determine the direction of a received signal by measuring the different delays between the received signals in the array. Although the concepts and terminology of this type of beam-forming are the same, it will not be further explored in this document. The term beam-forming used in the rest of the document will only refer to the manipulation of emitted beam-patterns.

The interference patterns are achieved when multiple transducers send slightly different signals between them. These interference patterns can be used with benefit by forcing the majority of the signal energy all in one angular direction. Typically this is done using weighted delays between the transducer signals.

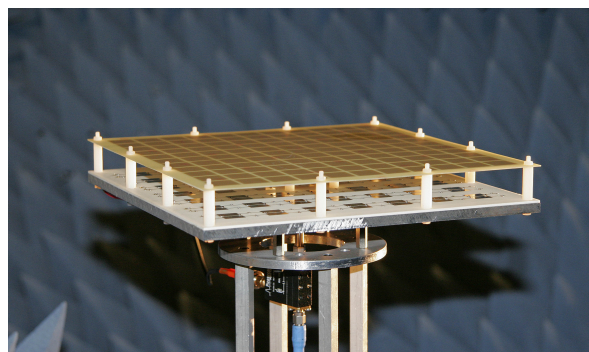


Figure 3.1: Example of a beam-forming directional antenna

Beam-forming techniques can be used either for radio waves as for sound waves. The

implementation of beam-forming in radio waves is used to create directional antennas to achieve higher power gains. One good example are the smart antennas which are focused in a specific area and therefore use some kind of beam-forming technique to focus their power in that area. A smart antenna array can change its beam pattern in response to the changing signals.

Some beam-forming techniques are also used in audio/ultrasonic waves. The ultrasound array is a well known application that takes advantages of the beam-forming techniques. Often used in many localization and mapping techniques, as referred in chapter 2, audible sound arrays are used in big music concerts to focus the sound in a specific area.



Figure 3.2: Example of a loudspeaker array

However beam-forming techniques are often used in sound applications, the direction control of the main power lobe is rarely done, at least in a dynamic way. This process is often called beam-steering, and can be defined as the controlled changing of the main lobe direction of a radiation pattern. It allows to focus the formed beam from an emitter array in several directions, instead of just the one perpendicular to the array plane (see figures 4.2(a) and 4.2(b)).

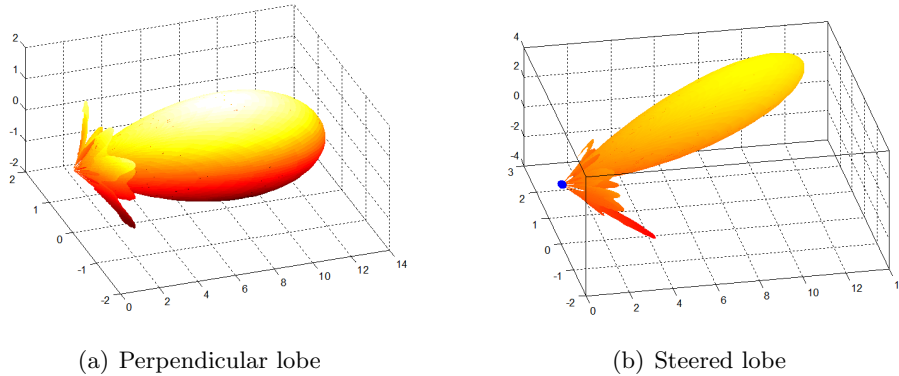


Figure 3.3: Beam-forming example

3.2 Beam-forming theory

A transmitting antenna, of either ultrasound or electromagnetic waves generates stronger waves in some directions than others. The field strength of the wave for every direction can be called the antenna's radiation pattern.

A wave measured at a point far from the antenna is the sum of the radiation from all parts of the antenna. Each small part waves travels a different distance to the point where a receiver is located. In some directions, these waves add constructively creating a gain. In some directions they add destructively losing power.

The resulting radiation pattern can be a very focused area. It has a narrow central *beam* of high gain and smaller beams, called *side lobes*, on the sides of the central beam. Directions in which the signal strength is zero are called *nulls*.

Beam-forming can be achieved using a relatively large surface emitter or a group of similar signal sources disposed in some pattern. The interference between the signals provides a space-filtering effect for the wave propagation in space. Consider without loss of generality that all the emitters are point sources and with omnidirectional power distribution in space. Consider also that there are no attenuation.

3.2.1 One dimension case - linear array

Let f be an omnidirectional wave emitter in the coordinate $x = x_f$ and P the point of reception at the coordinates (P_x, P_y) .

$F(x)$ represents the Fourier transformation of the emitted wave with wavelength λ in f .

$$F(x) = E(x)e^{-j\phi(x)} \quad (3.1)$$

where $E(x)$ is the wave amplitude and ϕ its phase.

In P , considering no attenuation, the function $F(x)$ at the distance l apart from the point f is and at a distance R from the reference origin:

$$F(x) = E(x)e^{-j\phi(x)}e^{-j2\pi l/\lambda}dx \quad (3.2)$$

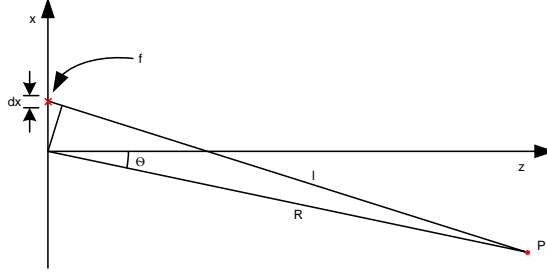


Figure 3.4: Construction for applying Huyghens' principle.

where the value l is given by equation 3.3

$$l = R + x_f \sin(\theta) \quad (3.3)$$

By Huyghens' principle[11] the result of a distributed emitter along the x axis will be the sum of the effects of all the infinitesimal elements. The resulting function, let's admit $P(x)$, can be written accordingly to the equation

$$P(x) = \int_{-\infty}^{+\infty} E(x) e^{-j\phi(x)} e^{-j2\pi l/\lambda} dx \quad (3.4)$$

$$P(x) = \int_{-\infty}^{+\infty} E(x) e^{-j\phi(x)} e^{-j2\pi(R+x_f \sin(\theta))/\lambda} dx \quad (3.5)$$

For the particular case of a infinitesimal point source, the result is greatly simplified to,

$$P(x) = E(x) e^{-j\phi(x)} e^{-j2\pi l/\lambda} \quad (3.6)$$

For a linear emitter array is disposed along the x axis at the positions x_n with N elements, as shown in figure 3.5, the group response can be given by the array-of-arrays rule. This rule says that the field pattern of a set of identical wave sources is the product of the pattern of a single wave source and the so called "array factor". This is done by convolving the emitter response and dirac impulses marking the sources positions along the axis.

The group resulting Fourier transform $L(x)$ is in equation 3.7.

$$L(x) = \sum_{n=0}^{N-1} E(x) e^{-j\phi(x)} e^{-j2\pi l_n/\lambda} \quad (3.7)$$

In the case of the far-field solution, when the point P is far enough to admit $l_n \gg d$, the different angle values between the direct line-of-sight and the z -axis have small variations. If those variations are ignored the several lines-of-sight can be seen as parallels. The result simplification is the case shown in figure 3.5.

Also, for θ values that are relatively small (let's say between 0° and 45°), if the distance d between emitters is much smaller than R , it is possible to admit that $R \gg r$ and the value of θ is equal for every emitter. This makes the approximation 3.9 valid.

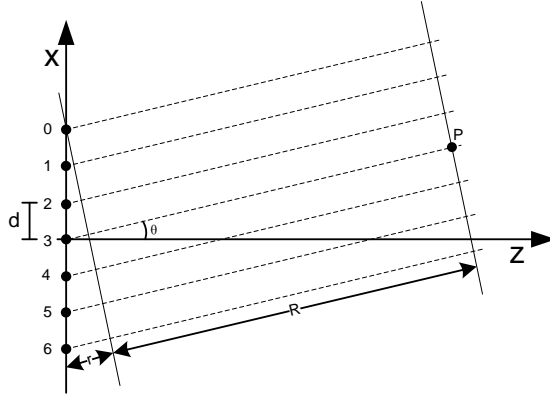


Figure 3.5: Linear emitter array simplified

$$l_n = R + r_n \quad (3.8)$$

$$l_n = R + x_n \sin(\theta) \quad (3.9)$$

This makes the solution for the far-field case equal to the following sum,

$$L(x) = \sum_{n=0}^{N-1} E(x) e^{-j\phi(x)} e^{-j2\pi R/\lambda} e^{-j2\pi x_n \sin(\theta)/\lambda} \quad (3.10)$$

This result is a generic simplification for a linear array of isotropic wave sources. If the sources are not isotropic but instead have a power spectral density in space given by the function $P_{emitter}(x)$ the resulting array power spectral density ($P_{array}(x)$) can be obtained. The superposition principle can be applied and the resulting function would be the one given by the equation 3.11

$$P_{array}(x) = P_{emitter}(x)L(x) \quad (3.11)$$

3.2.2 Two dimensions case - planar array

In the two dimensions case it is considered that instead of a linear array we have a planar array. The point of reception P now have the space coordinates (P_x, P_y, P_z) . The wave sources are now disposed in the xy plane arranged in a certain pattern. There are several array patterns that can be used, the most common are the rectangular and triangular pattern. However in some cases circular, oval or even random patterns are used. Some examples are shown in the figure 3.6.

For simplicity reasons we admit the use of a rectangular array pattern. The result can then be extrapolated to the other cases by changing emitter coordinates.

A two dimensions array can be interpreted as an array of arrays, this means a rectangular pattern array can be decomposed in an array along the y -axis of M elements that by themselves are arrays along the x -axis of N elements. See figure 3.7.

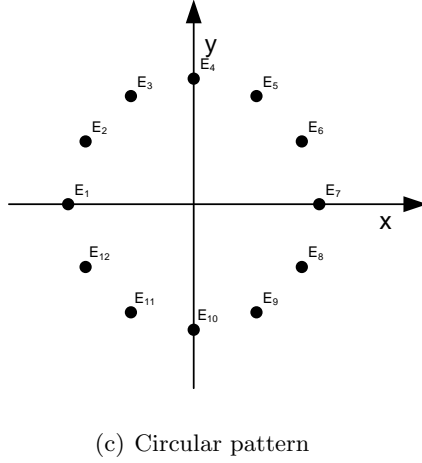
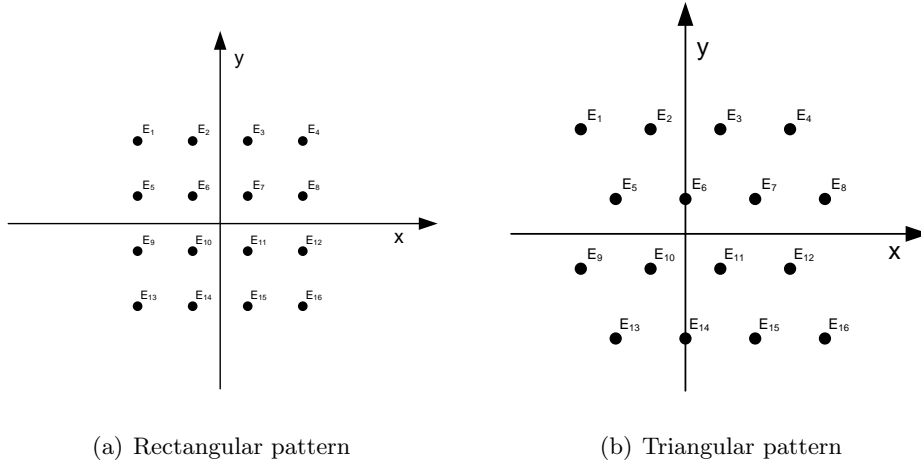


Figure 3.6: Array patterns

From the equation 3.12 a line of emitting sources in the x -axis can be viewed as only one emitter with the response $L(x, y)$ given by,

$$L(x, y) = \sum_{n=0}^{N-1} E(x, y) e^{-j\phi(x, y)} e^{-j2\pi R/\lambda} e^{-j2\pi x_n \sin(\theta_x)/\lambda} \quad (3.12)$$

Applying the same principle as earlier in 3.5 and 3.12 the array response $A(x, y)$ is,

$$A(x, y) = \sum_{m=0}^{M-1} L(x, y) e^{-j2\pi R/\lambda} e^{-j2\pi y_m \sin(\theta_y)/\lambda} \quad (3.13)$$

Replacing $L(x, y)$ the final solution comes,

$$A(x, y) = \sum_{m=0}^{M-1} \sum_{n=0}^{N-1} E(x, y) e^{-j\phi(x, y)} e^{-j4\pi R/\lambda} e^{-j2\pi(x_n \sin(\theta_x) + y_m \sin(\theta_y))/\lambda} \quad (3.14)$$

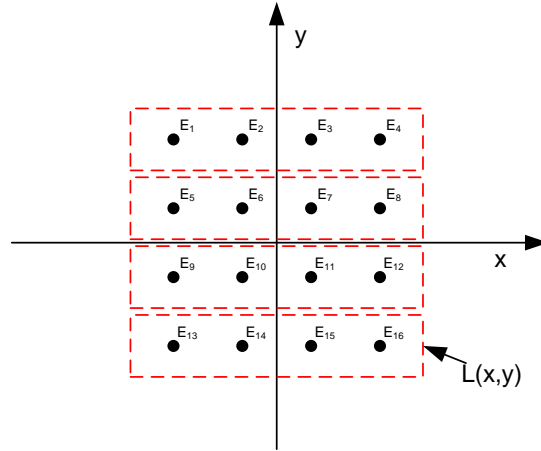


Figure 3.7: Rectangular array

where the positions (x_n, y_m) are the sources coordinates on the xy plane. Note that the coordinate system is not the typical spherical coordinate system, the value θ_x is the angle between the z -axis and the straight line from the origin to the point $(P_x, 0, P_z)$. Similar to θ_x , the value θ_y is the angle between the z -axis and the straight line from the reference origin and the point $(0, P_y, P_z)$ as shown in figure 3.8.

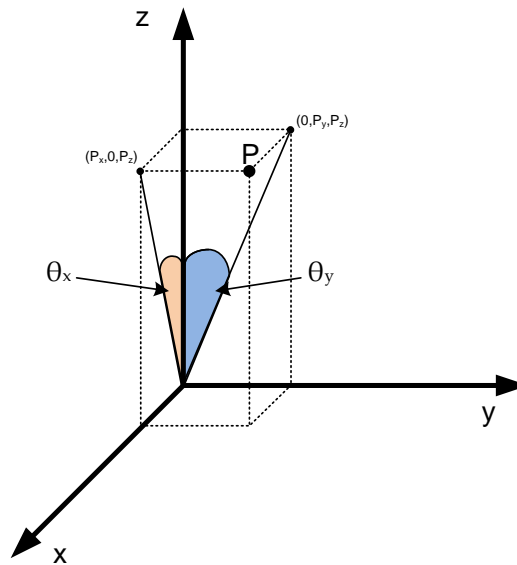


Figure 3.8: Used coordinate system.

For a more general case it is possible to admit that the array is a set of N emitters where the Cartesian coordinates of the emitter n are (x_n, y_n) and its individual Fourier transformation is the function $E_n(x, y)$. The equation 3.14 changes to,

$$A(x, y) = \sum_{n=0}^{N-1} E_n(x, y) e^{-j4\pi R/\lambda} e^{-j2\pi(x_n \sin(\theta_x) + y_n \sin(\theta_y))/\lambda} \quad (3.15)$$

Through the equation 3.15 it is possible to know the result power spectrum density from an emitter array in any point (P_x, P_y, P_z) . Alternatively, for a most simple use of the equation 3.15, the point P coordinates can be described in coordinates (R, θ_x, θ_y) .

3.2.3 Power spectrum in space

Using the obtained result in 3.15 the power spectrum of a particular emitter array can be determined. The figure 3.9 shows an example of a possible array with a triangular pattern and inter-element spacing of d .

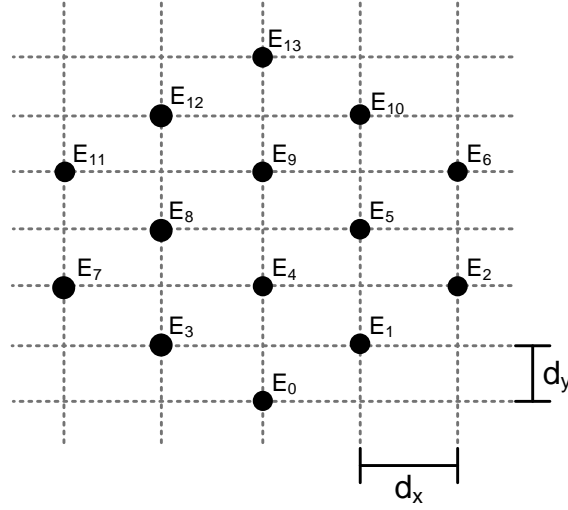


Figure 3.9: Example emitter array

Using a Cartesian coordinate system it is possible to define the distances d_x and d_y .

$$d_x = \frac{\sqrt{3}}{2}d \quad (3.16)$$

$$d_y = \frac{d}{2} \quad (3.17)$$

Computing the following equation 3.18 for all the values of n in the space defined by coordinates $(1, \theta_x, \theta_y)$ the power spectrum distribution figuring in 3.10 is obtained.

$$A(x, y) = \sum_{n=0}^{13} E_n(x, y) e^{-j\phi(x, y)} e^{-j4\pi R/\lambda} e^{-j2\pi(x_n \sin(\theta_x) + y_n \sin(\theta_y))/\lambda} \quad (3.18)$$

It is only considered the power spectrum in a cone of 30 degrees in front of the array plane.

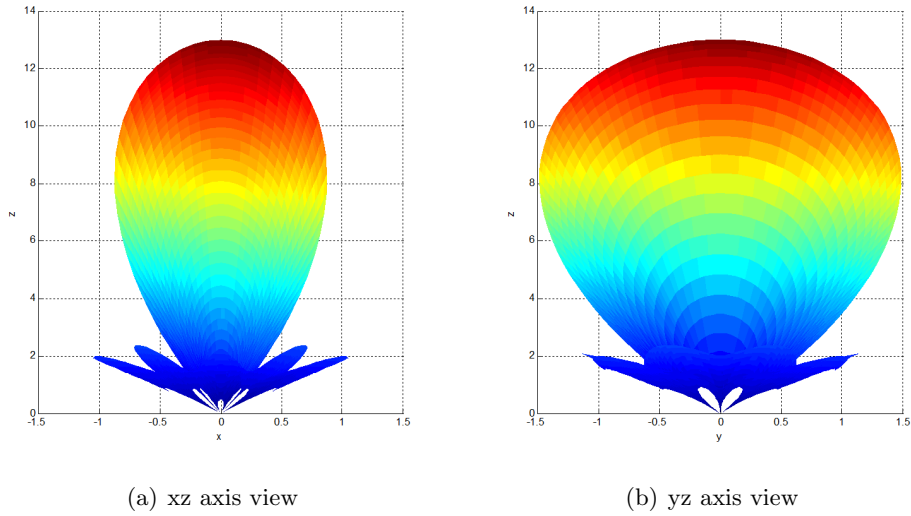


Figure 3.10: Power spectrum density

3.2.4 Directivity

The power density of an array emission can be analysed through its directivity. Directivity is an important measure because most of the power is intended to go in a particular direction. Also it permits to find in which direction the power is effectively being projected.

The directivity gain $D(\delta_x, \delta_y)$ in a certain direction for the coordinates (δ_x, δ_y) is,

$$D(\delta_x, \delta_y) = \frac{U(\delta_x, \delta_y)}{P_t/A_t} \quad (3.19)$$

where $U(\delta_x, \delta_y)$ is the radiation intensity in a direction (δ_x, δ_y) , P_t is the total radiated power defined as

$$P_t = \int_{A_t} U(\delta_x, \delta_y) dA_t \quad (3.20)$$

and A_t is the total solid angle containing all the radiated power.

As a comparative parameter, the directivity usually is compared to a perfect isotropic and it can be measured in dBi.

$$D_{dBi} = 10 \log_{10}[D] \quad (3.21)$$

3.3 Beam-steering

To effectively dynamically control the direction of the beam, a set of techniques often known by beam-steering have to be done. The beam-steering term refers to all the strategies that allow a beamed wave to change the direction of its main lobe, or even the secondary lobes. There are several applicable techniques either mechanical or involving some kind of signal processing.

The mechanical beam-steering techniques uses moving parts to control the physical orientation of the array. Usually using a servo-motor or other electro-mechanical way, this kind of beam-steering has no interest to be further analysed in the context of this work.

Most beam-steering mechanisms however use signal processing to achieve their goal. Although there are several ways to do the steer of the signal main lobe, all of them are based in the same concept. It is well known that the beam-steering can be seen as spatial filtering for a signal, usually this is done with the adaptation of a signal in both amplitude and phase for the different emitters. Combined amplitude and phase control can be used to adjust side lobe levels and steer nulls better than can be achieved by phase control alone[13].

However, for the far-field case, were the waves can be considered planar, the control of the wave-front direction is enough to steer the main-lobe. This allows a great simplification using only phase control of the emitter array.

Consider again the existence of N identical sources along the x axis with regular spacing between them and a desired wave-front deviated δ degrees from the z axis (See figure 3.11).

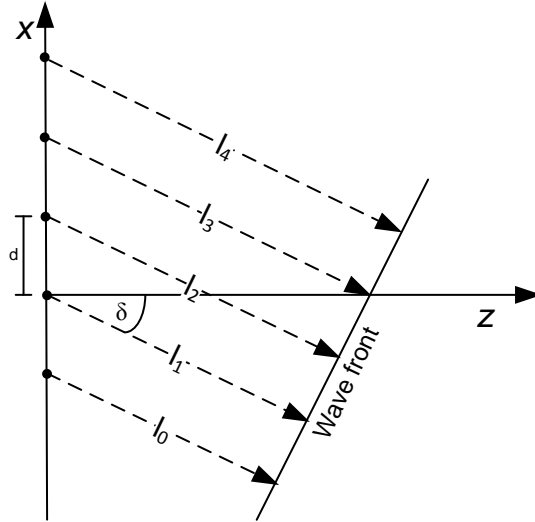


Figure 3.11: Steering a wave front

The necessary time for the waves to travel from the source to the wave-front plane are different for every emitter. In fact the time values are proportional to the distance l_n to the wave front.

As explained before in equation 3.9 these distances have a common factor when considering the far-field solution. Let l_n be the distance for the emitter n such that,

$$l_n = (t_n + t_0) \times c \quad (3.22)$$

where c is the propagation speed of the waves and t_0 is the minimum travel time between all the emitters.

$$R + r_n = (t_n + t_0) \times c \quad (3.23)$$

$$t_n + t_0 = \frac{r_n}{c} + \frac{R}{c} \quad (3.24)$$

The different time delays between each emitter for a desired wave front deviated δ degrees from the z axis are,

$$t_n = \frac{r_n}{c} \quad (3.25)$$

$$t_n = \frac{x_n \sin(\delta)}{c} \quad (3.26)$$

Extrapolating the result to the two-dimensions case is possible and simple when considering the far-field case. The necessary time delay is given by the sum of the time delay to compensate the deviation δ_y and the deviation δ_x . The final result is,

$$t_n = \frac{x_n \sin(\delta_x)}{c} + \frac{y_n \sin(\delta_y)}{c} \quad (3.27)$$

Note that similar to the coordinates used in section 3.2.2, the values δ_x and δ_y are measures along the same planes, but now accordingly to the desired steer direction.

The resulting power spectrum of a beam-steered emitter array using these delays is obtain trough the equation 3.15 adding the terms τ_n as phase delays.

$$A(x, y) = \sum_{n=0}^{N-1} E_n(x, y) e^{-j4\pi R/\lambda} e^{-j2\pi(x_n \sin(\theta_x) + y_n \sin(\theta_y))/\lambda} e^{\tau_n} \quad (3.28)$$

$$\tau_n = j2\pi(f \times t_n) \quad (3.29)$$

As an example a main lobe steer to the angle $(5^\circ, 10^\circ)$ would have the necessary delays given by,

$$t_n = \frac{x_n \sin(5^\circ)}{c} + \frac{y_n \sin(10^\circ)}{c} \quad (3.30)$$

For the same example array used in 5.17 the resulting power spectrum density would be as shown in figure 3.12.

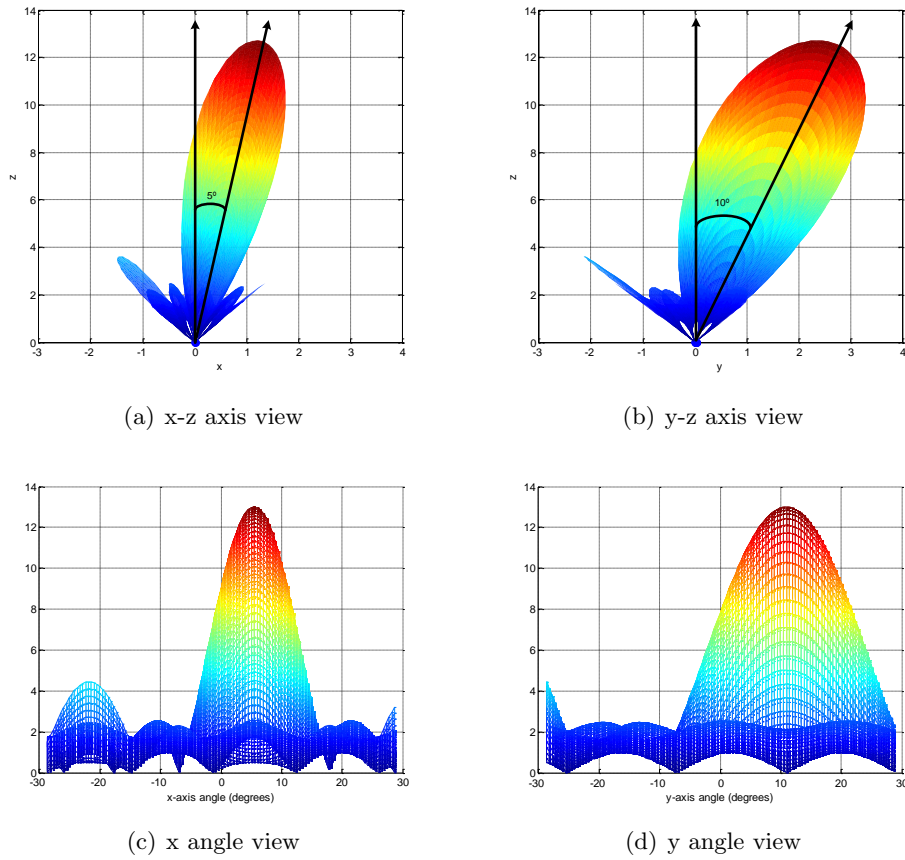


Figure 3.12: Power spectrum density with beam-steering

3.4 Digital Beam-forming techniques

The great majority of modern beam-forming systems exploit the advantages of digital implementations. The conversion is done filtering the analog signal to restrict the bandwidth to the interest frequency range and sampling the signal to the digital domain. The signal processing is usually using a digital signal processing unit (DSP) of some kind.

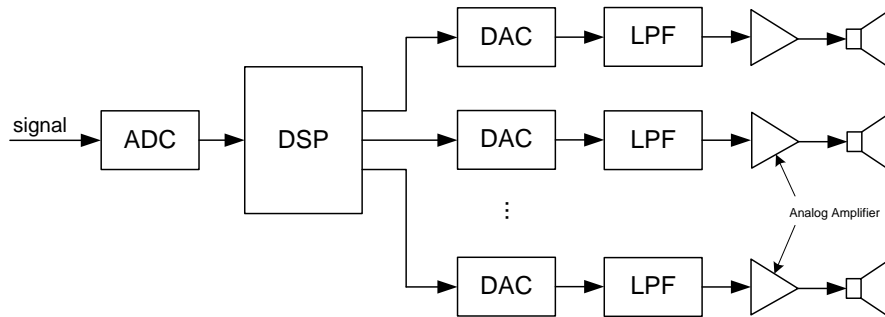


Figure 3.13: Typical beam-steering system

The commonly way to achieve the desired beam-pattern for a certain signal usually uses

some kind of digital signal processing. Typically a beam-former or beam-steerer linearly combines digital samples obtained through an ADC with the use of a digital signal processing unit (DSP). The main advantage of working in the digital domain is the easier signal manipulation using adaptive filters or algorithms.

The processing unit can be implemented in many different ways either using an hardware approach or a software approach depend on the goal application and signal frequencies.

3.4.1 Digital Beam-steering limitations

Although many techniques are viable, the key problem in using digital beam-forming with sampled signals is the need for non-integer delays. In the digital domain a discrete signal is obtained sampling a continuous signal. Converted by an ADC the discrete signal has an associated sampling frequency. Assuming that, if the frequency f_s satisfies the Nyquist sampling theorem the signal can be posteriorly reconstructed.

However the Nyquist sampling theorem doesn't guarantee the possibility of a precise beam-steering. To steer a beam in a particular propagation direction, the need emitter delays t_n are ideal values that, in general, are not integer multiples of the sampling period. Adding the delays to a discrete signal can only be done in multiples of its sampling frequency. This means the shortest delay t_0 achievable depends on the signal's sampling frequency.

$$t_0 = \frac{1}{f_s} \quad (3.31)$$

As analysed before in equation 3.26 there is a relationship between the angle to steer and the time delay. So to the minimum delay possible there must be a minimum steering angle (equation 3.32).

$$t_0 = \frac{x_0 \sin(\delta_0)}{c} \quad (3.32)$$

Replacing the value t_0 and admitting the value x_0 given by the inter-element spacing d we have the minimum or smallest steering angle possible δ_0 ,

$$\delta_0 = \sin^{-1} \left(\frac{c}{df_s} \right) \quad (3.33)$$

Equation 3.33 shows that the increase of the sampling frequency leads to a smaller steering angle which was expectable since the time delay resolution increases.

The common problem in real applications is that normal sampling frequencies, although respecting the Nyquist theorem, are too low to a satisfactory angle resolution. A practical example of such a case could be the beam-steering of the signal emitted by a parametric array. Consider the emitter array in figure 3.9 is a parametric ultrasound array emitting a modulated signal around a frequency of 40kHz. The spacing values are $d_x = 7.8mm$ and $d_y = 4.5mm$.

Considering the worst case in terms of minimum delay and the speed of sound propagation given by $c = 343m/s$ the minimum steerable angle is,

$$\delta_0 = \sin^{-1} \left(\frac{343}{f_s \times 4.5 \times 10^{-3}} \right) \quad (3.34)$$

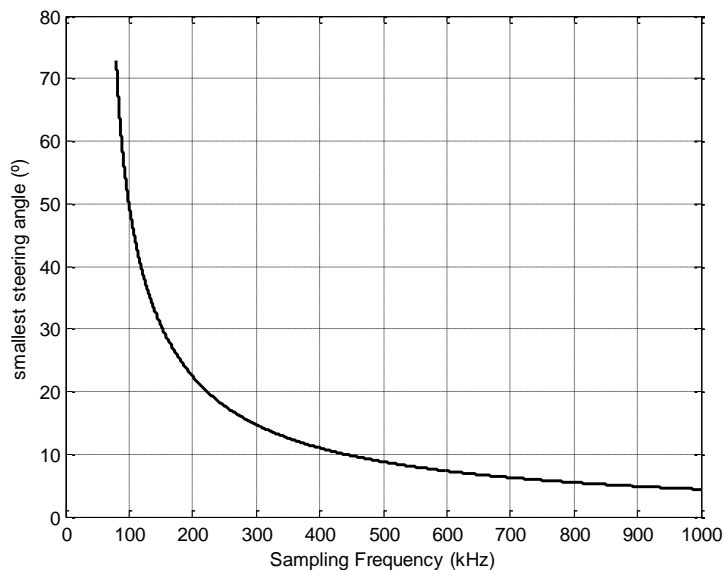


Figure 3.14: Variation of the smaller steering angle with sampling frequency

Testing a set of possible sampling frequencies, from 96kHz to 1000kHz, that respect the Nyquist theorem, the minimum steering angle possible in degrees is displayed in graph 3.14.

In this application, as it is possible to see, for a reasonable high sampling frequency, let's admit 192kHz, the minimum steering angle still is too big. In fact for a 192kHz sampling the steering angle is,

$$\delta_0 = \sin^{-1} \left(\frac{343}{192 \times 10^3 \times 4.5 \times 10^{-3}} \right) = 23.39^\circ \quad (3.35)$$

For a precise beam-steering 23.39° as a minimum steering is a very high value not allowing a good angle resolution.

The following table shows the relations between the commonly used sampling frequencies and the smallest steering angle achievable for this array disposition.

Sampling frequency	Smallest steering angle
96.000 Hz	52.56°
128.000 Hz	36.55°
176.400 Hz	25.60°
192.000 Hz	23.39°
320.000 Hz	13.78°

Table 3.1: Smallest steering angles for common sampling frequencies in sound applications.

The impossibility of a high angle resolution beam-steering with common sampling frequencies is well perceptible viewing these smallest steering angles. Several techniques try to overcome this limitation of the sampling frequency. The following sections will expose some solutions to resolve this problem. Two distinct types of approaches are done, the time-domain techniques and the frequency-domain techniques.

3.4.2 Time domain techniques

The simplest digital time domain beam-former is shown in figure 3.15. The original signal is sampled using an ADC at a sampling frequency f_s . To reduce the loss of beam integrity created by delay quantization in a sampling signal, we can upsample the ADC signal by L using an interpolation stage. Because the upsampling introduces replicas of the original frequency spectrum in f_s multiples, the signal has to pass through a low-pass to eliminate them.

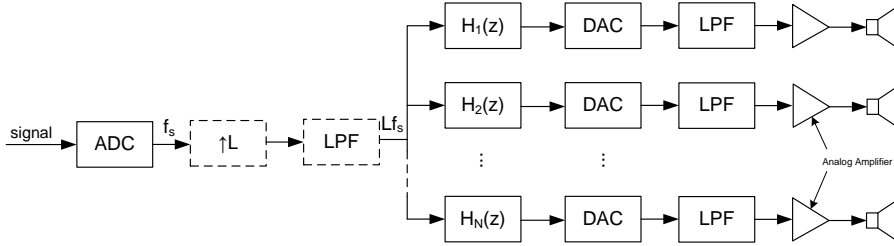


Figure 3.15: Beam-steering system in the time-domain.

The weighted delays for every different emitter are in fact achieved using the bank filters $H_n(z)$. For a great majority of the practical applications these delays are in reality delayed samples, however a more complex filter can be implemented using FIR filters. Because these filters are linear, it is possible to interchange or join the low-pass filtering and the beam-forming/beam-steering operation.

3.4.3 Frequency domain techniques

With discrete-time beam-forming the digital processing unit can also be used to compute algorithms that use the frequency domain to realize a beam-steering system. Even more, discrete-time beam-formers implemented in the frequency domain have sometimes superior characteristics compared to time-domain alternatives.

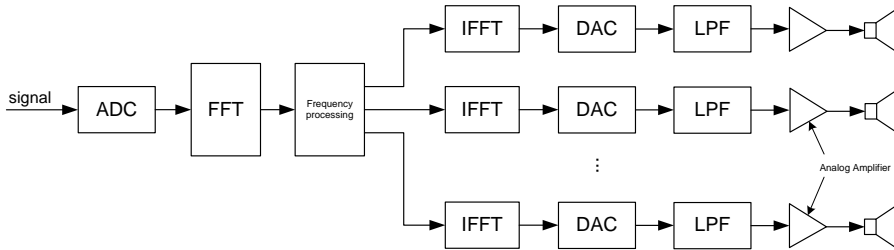


Figure 3.16: Beam-steering system in the frequency-domain.

Usually these systems use a short-time Fourier analysis of the sampled signal in a time window composed by N samples. A Fast Fourier Transform (FFT) algorithm can be used to obtain a frequency representation of the original signal. The signal then can be changed inserting the desired delays for each output, leaving to the existence of several different frequency representations. These frequency signals must be changed back to the time domain using a Inverse Fourier Transform (IFFT) for each output.

The use of such a method find its main disadvantage in its complexity. Because a large number of operations are necessary to realize the FFT and IFFT operations, the need re-

sources are typically too cumbersome to implement a implement low-cost solution in practical applications.

Chapter 4

System specifications and simulation

4.1 Introduction

The following chapter presents and describes the projected system at system level done in this work. Only considering the beam-steering implementation challenge this chapter is divided in three distinct sections. In the first section the system requirements and specifications are defined. The second section explains the method approach used and its advantages when compared with others. In the second section no specific hardware approach will be done, leaving it for the next chapter. Finally in the third section the results from system simulation are shown.

4.2 System objectives

The proposed system has the main objective of a steerable beam using a parametric array. The steering capacity should be achieved through a beam-forming and beam-steering technique that allows a precise beam-steering. The goal set to the project was to use an angle resolution in which the minimum angle was between 1° and 2° .

Additionally, the beam-steering technique should allow a real-time steering. This means not only that the steering shouldn't be fixed for a certain setup, but also that the main lobe direction changing have to be fast and with no beam deterioration. This beam-steering is controlled by the user who has to enter the steering angles in the system. For every other operations the hardware should be considered as a black box to the user.

The proposed system uses an ultrasound parametric loudspeaker, disposed in a planar array with a triangular pattern (figure 4.1), that reproduces intelligible sound using the parametric loudspeaker phenomena. To that, the ultrasound transducers will send a 40kHz phase modulated wave.

This design solution was found to be a very compact and efficient use for this particular case and frequencies. However the background concept can be applied to other cases where a precise real-time beam-steering is necessary.

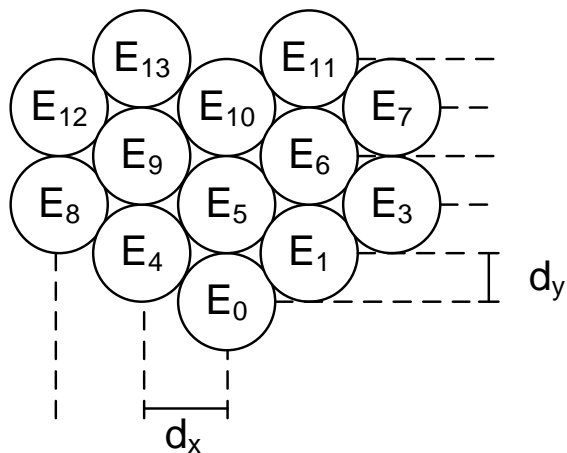


Figure 4.1: Ultrasound array pattern

4.3 System delay method

The proposed method tries to surpass the sampling frequency limitations in a beam-forming system without a great increase of the system complexity and cost. As explained before in this document the main limitation in digital beam-forming/beam-steering is the sampling frequency that, more often than not, isn't high enough to a precise steer. This lead to the need of upsampling methods in interpolation beam-forming or more complex solutions that use the frequency domain.

Because many practical beam-formers are in fact complex digital processing systems, the used method in this project greatly emphasizes the hardware simplicity and cost. It tries to achieve a beam-steering technique that leads to a low-cost and simple hardware implementations, with no loss of reliability when comparing to the more common counterparts techniques.

The main idea behind this system is the use of a naturally high frequency in a sigma-delta modulator (SDM). Although usually the increase of the sampling frequency doesn't bring more simplicity to the system, when it is a natural characteristic of the system it could be explored.

Consider the previous example in the equation 3.35 now for higher frequency levels using an oversampled SDM.

The SDM output frequencies are typically much higher than the original sampled signal, originating in consequence a smaller steering angle.

The figure 4.3 shows the block diagram of the considered system. For simplicity reasons it is assume that the source signal is already the signal to be steered and that no extra modulation (considering the parametric array case) is necessary.

The system can be divided in 3 different blocks. The first one is the interpolator and the SDM. The sigma-delta modulation trades a n -bit resolution at a sampling frequency f_s with a 1-bit resolution at a higher sampling frequency f_{us} .

The resulting signal is then processed in filter network. Because the signal now only has 1 bit per sample, the filter banks are very simple. In fact it can be reduce to a simple 1-bit

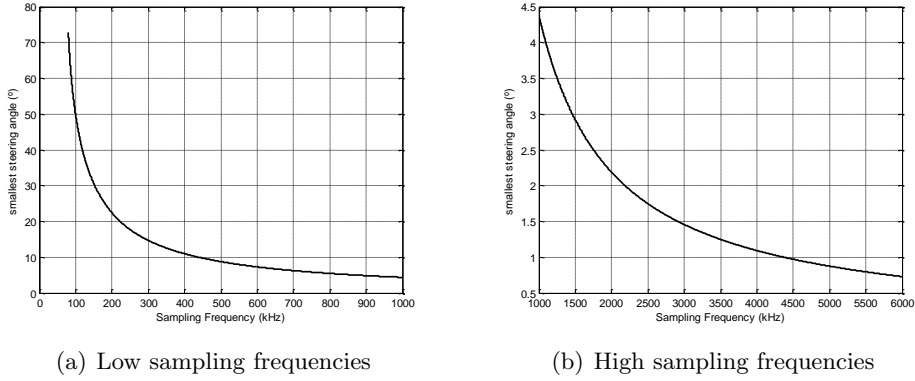


Figure 4.2: Steering angle depending the sampling frequency

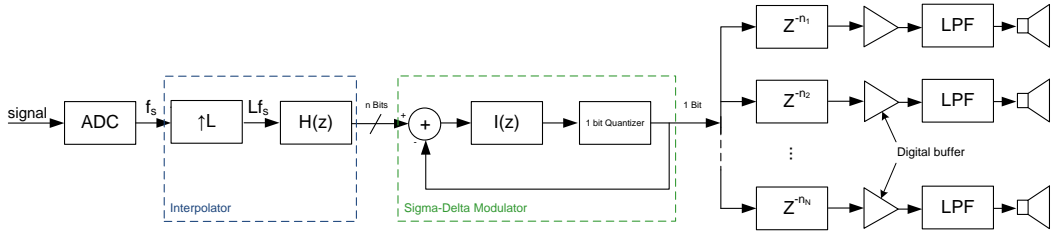


Figure 4.3: Proposed system block diagram.

delay chain.

Lastly, the output stage, is responsible for the signals amplification and filtering. The output signal of the delay bank will be a group of delayed sigma-delta signals. From the functionality point of view, these signals are in fact the as valid as the output of the SDM. This means it can be used to reconstruct the original signal with just a low-pass filter.

Further details in each different blocks are in the following sections 4.3.1, 4.3.2 and 4.3.3.

4.3.1 Sigma-delta modulator and upsampling

Sigma-delta modulation is usually known as a method for encoding analog signals into digital signals. Other common use for the sigma-delta modulation is the conversion of higher-resolution digital signal into a lower-resolution one, also digital. The conversion is done using error feedback, measuring the difference between the input and output signals (see figure 4.4). The lower-resolution output has a higher changing frequency than the input. This way the output signal can be filtered to recover the original signal without any loss of fidelity[14].

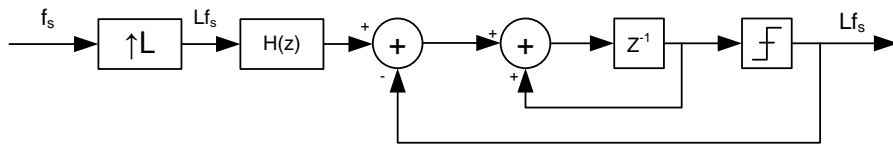


Figure 4.4: First order sigma-delta modulator with 1-bit resolution output.

The sigma-delta modulator model used is a first order modulator preceded by a signal interpolator. The interpolation stage oversamples by L the original signal so that the sampling frequency in the SDM output are sufficient to reconstruct the original signal.

The use of a sigma delta modulator does a up-sampling in the system sampling frequency. However the system complexity doesn't grow as much as in the previous examples. The first simplification is that the forwarding signal is only a 1-bit stream. This makes a simpler delay network as the next section will show.

The SDM is often used as a compact DAC implementation in many digital circuits. The low hardware requirements often make it a cheaper choice for many applications including in audio use. Not being exactly considered a DAC in its most primal definition, the SDM used in this method acts in fact as a DAC. Although the SDM output still is used in the digital domain by entering the delay network, the signal is in fact sigma-delta modulated and can be used at any time to reconstruct the original signal. Thus, using this technique the delay network output signals can be immediately used to reconstruct analog signals using just a simple low-pass filter, which brings the benefit of need no more DACs for the output signals. A common beam-forming system needs as many DACs as the system outputs number, while this method makes only needed one SDM for as many independent outputs as needed.

The working frequency of the sigma-delta can be defined trough the oversampling ratio necessary to maintain the signal quality. Oversampling is simply the act of sampling the input signal at a frequency much greater than the Nyquist frequency. Oversampling decreases the quantization noise created by the 1-bit quantization at the output of the SDM. Sigma delta modulator often requires 64 times sample rate to represent the signal, however largest values of L are used to eliminate quantization noise in the lower frequencies.

4.3.2 1-bit delay network

The output signal received from the SDM is a 1-bit stream at a frequency f_{us} , because it is a 1-bit signal the applied filter are very simplified eliminating the need for a more complex filter. Thus, a real-time beam-steering uses filters with changeable parameters. Usually, when FIR filters are used, the filters coefficients are changed for an appropriate response, those are commonly called adaptive filters. Choosing the appropriate delays using a 1-bit delay network comes as simple as choose the right number of sample delays to use in a delay chain. A very simple hardware approach to this delay network using multiplexers is explained in the next chapter.

The discrete sample delays Δ_n have a direct relation with the continuous time delays t_n , in fact the values t_n are integer values of the upsampling time such that,

$$t_n = \frac{\Delta_n}{f_{us}} = \frac{\Delta_n}{Lf_s} \quad (4.1)$$

4.3.3 Output stage

Usually beam-forming systems have an high number of outputs. In most designs it implicates the use of an high number of DACs. This can be very cost expensive and uses a lot of resources in real applications.

The proposed design joins all the necessary DACs in just one SDM. The signals obtained trough the delay network are all sigma-delta signals. This means that using just a low-pass

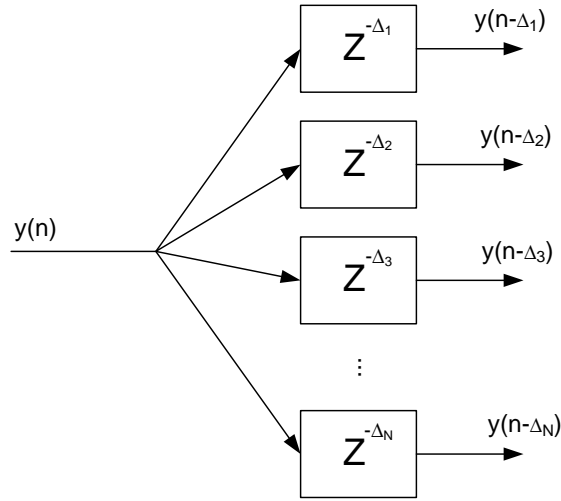


Figure 4.5: Delay network.

filter the original signal can be reconstructed. By using only one SDM instead of many DACs the costs can be highly diminished.

Other advantage is the signals amplification. To actually drive a load (such as an ultrasound transducer) in any practical system there is the necessity of an electronic amplifier. When using a sigma-delta signal on the output the amplification stage can be simplified to the use of a digital buffer in a class D amplifier. Since the signal have only two levels before filtering, the amplification can be done digital using a digital buffer.

The resulting two-level output signal contains the desired signal, but also higher frequency components. These added frequency components arise from the quantization error of the delta-sigma modulator, but can be filtered away by a simple low-pass filter. The result is a reproduction of the original, desired analog signal from the digital values.

4.4 Simulation and beam integrity

Before the method implementation some specifics of it were tested. The simulations' result was the produced beam for the different conditions. Previously to the system conditions test, a ideal case was tested using very precise delay values and considering that there were no errors in the transducers positioning.

The simulations were made using MATLAB 7.12. We considered that, all the transducers are perfect isotropic emitters with a wave frequency of 40kHz and always considered as point sources, also the test points were all in the far-field. The global spacial power spectrum density was computed using the equation previously obtained in 3.29 with the objective of seeing the result beam deterioration for several parameters.

For reference, none of the simulations takes in consideration for the parametric array phenomena. The emitted waves are ultrasonic but no demodulation process is considered. Only the space power density spectrum is measured and considered.

4.4.1 Ideal case

If the sampling frequency was as high as needed, the necessary time delays to do the beam-steering of an array could be exact. This leads to a perfect steering at any angle, which in practice is impossible, however it could establish a standard to compare the system performance.

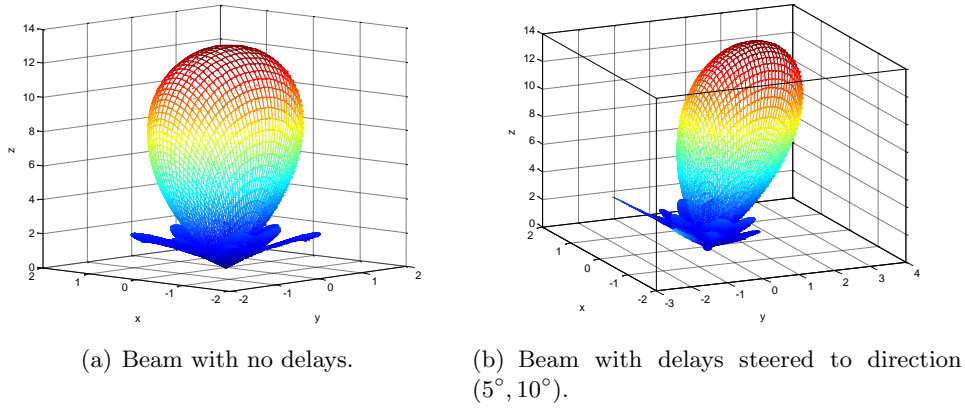


Figure 4.6: Beam-forming with exact delays.

For reference purposes figure 4.6 shows the resulting ideal beam simulated using MATLAB.

4.4.2 Delay quantization

In real applications the digital system is always limited by a sampling frequency. How this limitation affect the beam-steering can vary for the steering angle chosen. By the equation 3.33 it is known that the minimum steering angle is limited by the inter-element spacing in the array and the sampling frequency.

Accordingly to the graph in 4.7, to achieve the goal angle resolution (between 1 and 2 degrees), the sampling frequency must be between 2200kHz and 4400kHz.

To test the produced beam integrity for several sampling frequencies, its directivity gain was computed accordingly to the equation 3.21. Because for a specified frequency the directivity is differently affect for different steering angles, the directivity values are in fact the mean of a grid of steering values between -20° and 20° in both directions and spaced between them by 4° .

The results are graphically displayed in figure 4.8.

4.4.3 Position error

The physical realization of the array can have some positional errors. The main cause could be small assemblage errors mounting the components. If the ultrasound transducers positions are not precise and in the expected place, the delays calculations can be wrong and the beam could lose its integrity.

These errors can happen in every direction, so positional aleatory errors were considered in the transducer positions with a mean value between 0mm and 2mm in all Cartesian coordinates.

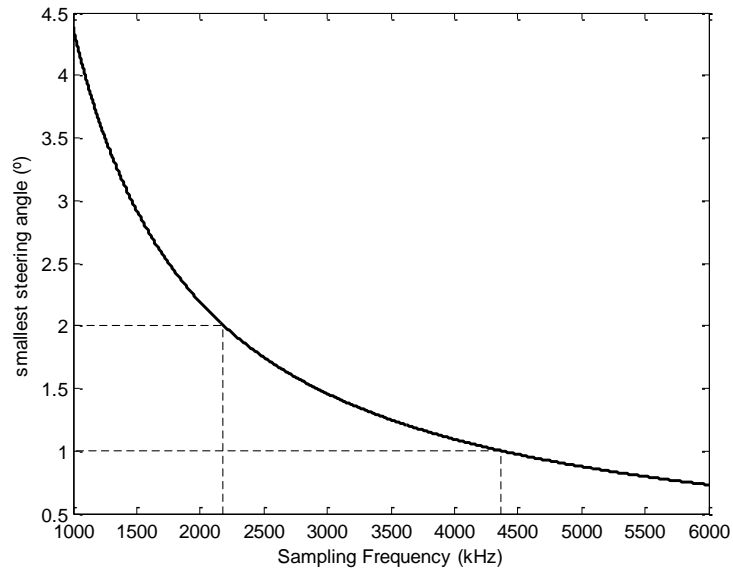


Figure 4.7: Steering angle depending the sampling frequency.

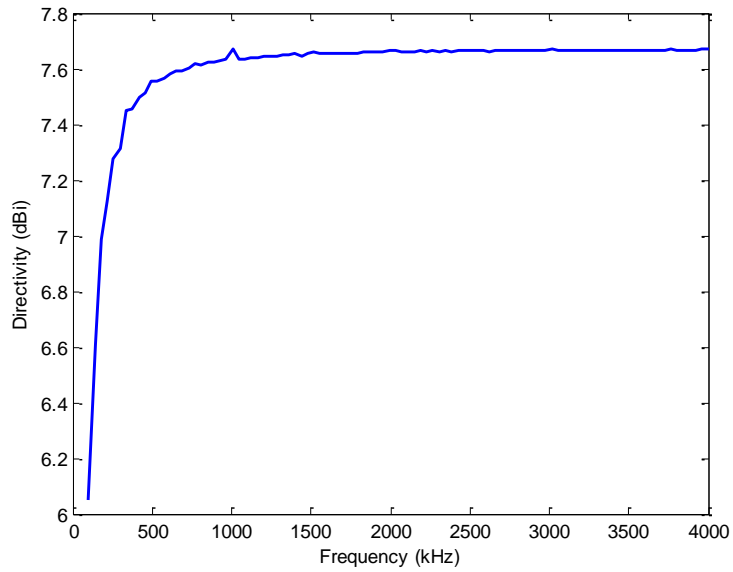


Figure 4.8: Directivity depending the sampling frequency.

The results are graphically displayed in figure 4.9.

As expected, the higher the position error the lower the array directivity is. However, for typical hardware assembling error, that it is less than 0.5mm, the loss of directivity is very small. Normal assembling techniques should be precise enough to despise the introduced position error in this particular application.

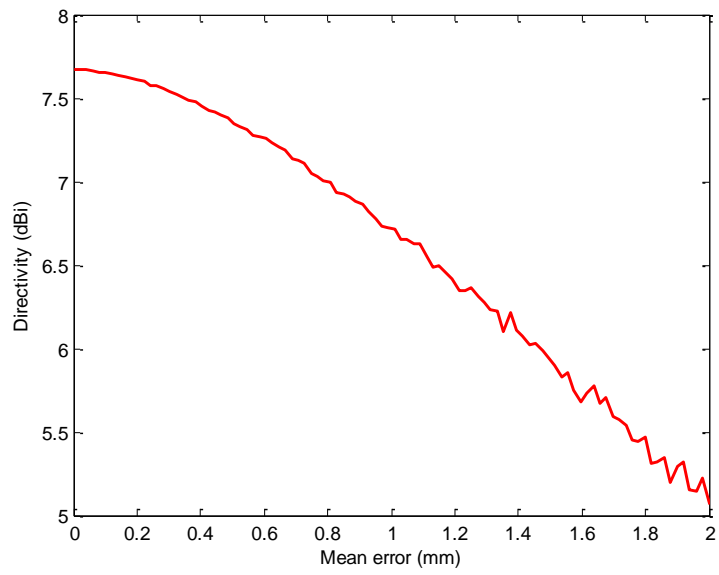


Figure 4.9: Directivity depending the positioning errors.

Chapter 5

System design

5.1 Introduction

In this chapter the implemented system hardware will be dealt. Using the previously defined system specifications, the several hardware solutions will be presented and justified.

Taking advantage of the natural high frequency used in a sigma-delta modulation is the fundamental concept leading the hardware design chosen. It uses the SDM followed by shift-register based delay selection for the different output. The system was implemented using reconfigurable hardware in a FPGA joined with a micro-processor for a simpler user from the user point of view.

The use of FPGA lead to a great freedom in hardware design making a very simple and compact solution possible allied to the needed reconfigurability in several hardware parameters.

The next section shows a top level approach of the hardware implementation and divides it in sub-systems to be explained in the following sections of this chapter.

5.2 System top level view

The system was implemented in a development board from Trenz, the GigaBee XC6SLX with Spartan-6 FPGA from Xilinx additionally with an expansion baseboard also from Trenz. The majority of the system hardware was implemented using VHDL except for the use of an embedded Microblaze processor as system controller to provide a user-friendly environment. The software approach to this controller will also be described in this chapter.

The choice of a FPGA to the project comes from several factors. The FPGAs are a very powerful technology for developing hardware systems. This is because the FPGAs are in fact reconfigurable hardware making it a cheap alternative when testing different digital hardware approaches. It allows the chance of fast prototyping with fast design cycles and no high risks associated. This and the possibility of introducing debug hardware to help the hardware development are good reasons to use FPGAs.

Other reason for FPGAs the use is strict timing characteristics that this kind of hardware have. When designing a system where the relative system timings must be precise, a sequential machine such as a micro-controller doesn't have the necessary time guaranties.

Finally the Xilinx FPGA development tools provide a simply configurable processor that can be used as a simple, easy understandable and easy configurable interface between the

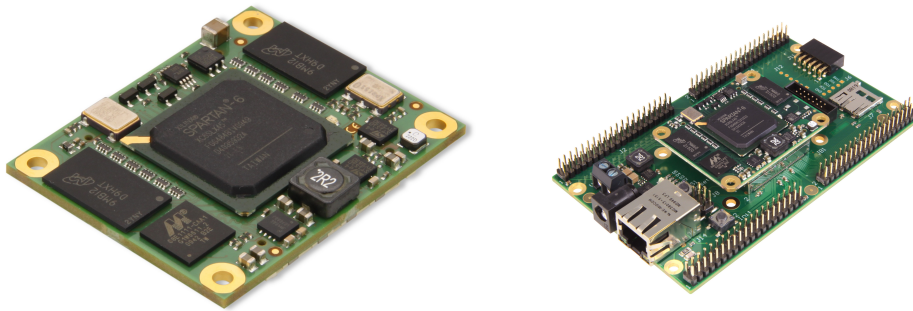


Figure 5.1: GigaBee XC6SLX board and baseboard.

hardware and the user.

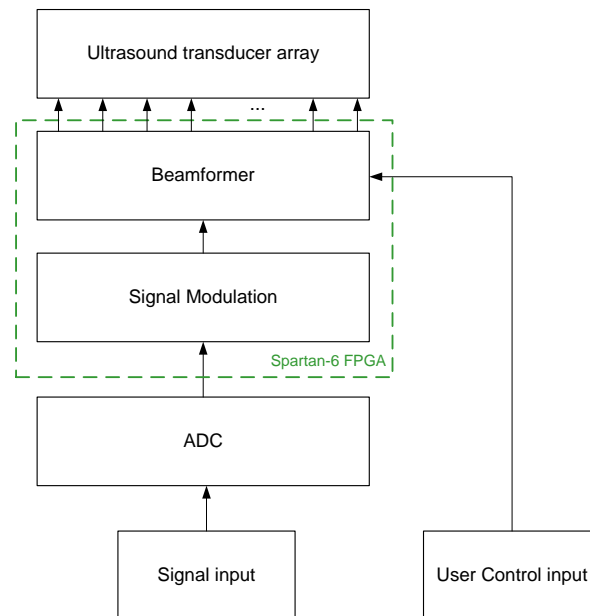


Figure 5.2: Top level view of the implemented system.

The developed system was divided in 4 distinct blocks (see figure 5.2). The ADC block is responsible for the signal acquisition translating the analog signal to a digital representation. Then a signal modulation block modulates the source signal with a ultrasound carrier. The third block is the beam-former, where the beam-forming control is done accordingly to the user inputs and the pre-determined array dimensions. Finally the transducer array is responsible for the signal amplification and transmission. A more complete and detailed view of these blocks are done in the next sections.

5.3 ADC

For the signal acquisition it was used the Digilent PmodAD1 (figure 5.3). It is a module converter board that uses a PMOD connector, a small I/O interface that offer extended

capabilities for FPGA boards. The board have two AD7476A 12-bit A/D converter chips and two 2-pole Sallen-Key anti-alias filters with poles set to 500 KHz, allowing 2 simultaneous parallel conversions. For more detailed information about the board and conversion chip see [15] and [16] respectively.

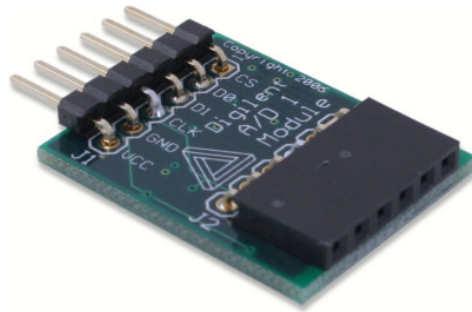


Figure 5.3: Digilent PmodAD1.

Although two simultaneous conversions can be done, in the implemented system it is only used one of the chips because only one output signal is used. The sampling frequency of the ADC can go up to one million samples a second, however because the sampled signal is in the audible band, this is 20Hz to 20kHz, the sampling frequency was set to 250kHz.

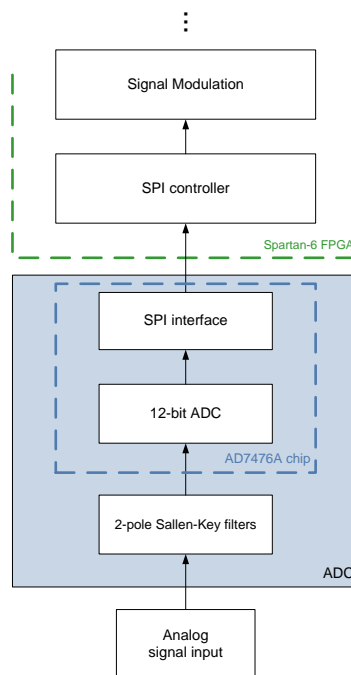


Figure 5.4: ADC block.

The acquired signal is passed to the FPGA board using a SPI interface. In the FPGA the SPI interface controller was programmed in VHDL using a finite state machine accordingly to the serial interface protocol defined in [16].

5.4 Signal modulation

The main function of this block is to modulate the acquired signal so that the air demodulation produces an audible beam. In section 2.3 some techniques to modulate the signal were referred and explained.

All the possible modulations (this is AM-SSB, AM-DSB, PM and FM) were tested using the MATLAB Communications System Toolbox and a commercial ultrasound array produced by Nicera.

The modulation that shown a perceptible better quality in the demodulated signal was the phase modulation. Note that the term quality refers to the demodulated sound that seems the most pleasant to the human hear and more similar to the original audio sound reproduced by common loudspeakers. The relation between this "quality" and the existence of harmonic distortion exists as explained in section 2.3, however it is not measure in any quantitative scale in this project.

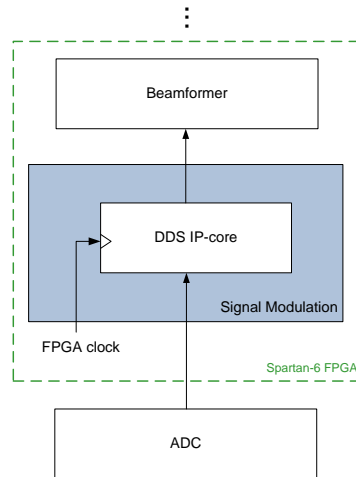


Figure 5.5: Signal phase modulation block.

From the hardware programmer point of view, along with FM, PM have the easier implementation using a FPGA. The phase modulator was implemented using a direct digital synthesizer (DDS) which is a type of frequency synthesizer constructed with base on a frequency reference and a numerically controlled oscillator (NCO).

The DDS used, the LogiCORE IP DDS Compiler v4.0, is a hardware IP-core from Xilinx with many configurable parameters. For further details see the IP-core data sheet[17].

Despite the many options possible for the DDS compiler, the used system is much simpler. It uses the phase accumulator set to generate a 40kHz periodic signal. The phase from the phase accumulator is then summed to the ADC signal in the POFF_IN port generating the real wave phase. This phase is used in the look-up-table (LUT) to generate digital sine signal with 40kHz and phase offset controlled by the 12-bit ADC signal

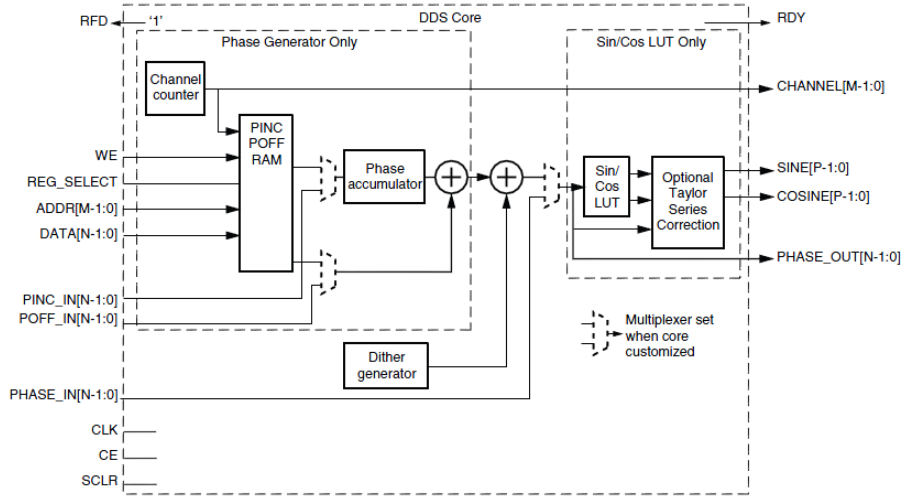


Figure 5.6: DDS core architecture.

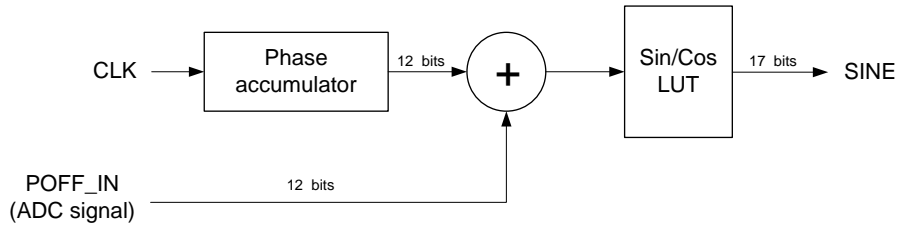


Figure 5.7: PM modulator.

5.5 Beam-former hardware

The beam-former is the system block responsible for the control in real time of the ultrasound beam main lobe. It receives the intended direction in degrees and makes all the necessary calculations to project the wave front in that direction. The hardware can be subdivided in 3 parts as the figure 5.8 shows.

5.5.1 Sigma-Delta DAC

In section 4.3.1 a sigma-delta modulation was proposed (see figure 5.9).

The interpolation stage has the objective of up-sampling the original signal to the frequency used in the SDM. For implementation simplicity this block can be reduce to a trivial block when considering that the filter $H(z)$ is a zero order hold filter. These filters basically hold the last value read during the original signal sampling time, then reads the next digital sample and holds that signal for the sample time as well.

In terms of hardware the zero order hold filter is nothing more than a data register that is written at a sampling frequency f_s and read at a L times higher frequency f_{us} . This makes the interpolation stage as simple as a bus connection if the ADC output is registered. In case of a non-registered output the interpolation is a data register with a clock supplied by the ADC.

The input signal in the sigma delta comes from the signal modulation block. The number

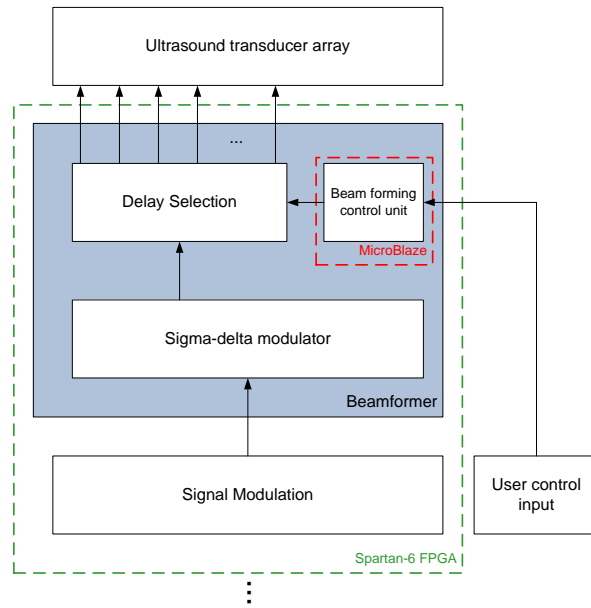


Figure 5.8: Beam-former hardware.

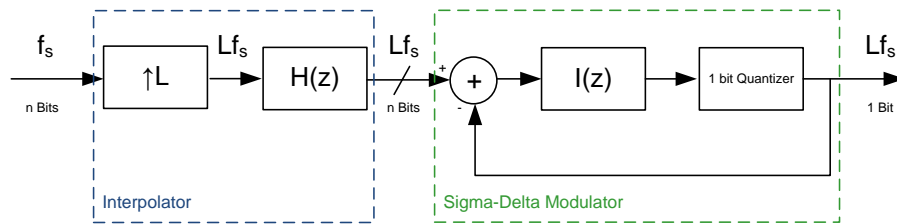


Figure 5.9: Sigma-delta modulation.

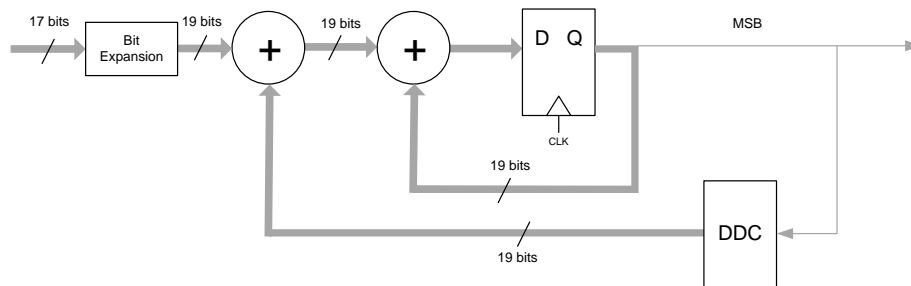


Figure 5.10: Implemented sigma-delta modulator.

of bits in this signal is defined by the precision intended in DDS. In this particular case the signal has 17 bits, however to avoid loss of signal due to the binary additions carry, there is a 2-bit expansion block in the SDM input.

The integrator $I(z)$ is in fact a digital integrator composed by a data register and a sum between its input and output.

The SDM internal signal are in two's complement, meaning that the integers range is -2^{19}

to $2^{19} - 1$, however the input signal integers range is -2^{17} to $2^{17} - 1$. The expansion bits are applied in the left of the remaining bit word meaning their now are the most significant bits and their value is the same of the previous MSB so that the value in two's complement doesn't change. The external feedback levels that are going to be compared with the input must be set to -2^{17} to $2^{17} - 1$. The DDC unit stands for Digital-to-Digital converter and is similar to a quantizer but not changing the used bit length. The DDC analyses the most significant bit(MSB) in the integrators output, if it is '1' the signal is negative and the feedback value is -2^{17} , else if it is '0' the output is a positive signal and the feedback is $2^{17} - 1$.

When using the MSB of a two's complement signal as output, it should be negated so that to positive integer (MSB is '0') corresponds a high voltage value and to a negative integer (MSB is '1') corresponds a low voltage value.

The working frequency of the sigma-delta modulator was set accordingly to the limits to achieve the desired angle resolution, between 1° and 2° . The chosen frequency was 4MHz, that is in the established limit of 2200kHz and 4400kHz defined previously.

Higher order sigma-delta modulator

In the final project we used a first order sigma-delta modulator, however the use of higher order SDMs can be done. To obtain a better signal to quantization noise ratio, high order SDMs are recommended. A study to a parametrizable implementation in terms of order and passing-band using a CIFB structure was made and can be found in appendix A.

5.5.2 Delay Selection

Accordingly to the subsection 4.3.2 the transducers' delays can be achieve with a 1-bit delay network. To reach simpler and more compact hardware solution, the delays come from a 1-bit serial-in, parallel-out shift-register(SR). The sigma-delta modulator feeds the bit stream to a serial input in the shift register while all it's outputs can be read at any time.

The shift-register clock frequency is exactly the same as the sigma-delta modulator, in fact at the hardware level the clock signal is the same for both entities. This way the shift-register does a shift for every new sigma-delta sample.

If the SR has a length of M bits in it's parallel outputs, the last M samples from the sigma-delta modulator are available. Choosing a right combination between frequency and the shift-register length it is possible to achieve the delay values of t_0 and t_{max} defined in section 4.3.2.

In fact for the specified conditions the value M is,

$$M = t_{max} \times f_{us} \tag{5.1}$$

$$M = \frac{x_{max} \sin(\delta_{max}) f_{us}}{V_p} \tag{5.2}$$

$$M = \frac{45\text{mm} \times \sin(30^\circ) \times 4\text{MHz}}{343\text{m/s}} \approx 262 \text{ samples} \tag{5.3}$$

The number of samples is perfectly achievable using a FPGA, in truth, the value used was 512 samples. In terms of FPGA resources used, the length of the shift-register is equal to the number of flip-flops used. To a common Spartan-6 FPGA the use of 262 flip-flops represent

a small percentage of the available ones, which means that doubling the used flip-flops will not represent a negative impact in the used resources.

The value 512 was preferred because the parallel SR outputs will need to be addressable. To address a set of 262 individual ports it is necessary 9 bits however 9 bits are capable of addressing a total of 512 different outputs.

Other advantage for a posterior export to a bigger array, this is with more transducers and therefore a bigger value of x_{max} and t_{max} , is that use of a SR with 512 outputs makes no need of any change in the shift-register.

With all signals, delayed from t_0 to t_{max} and space between them by t_0 , available in the shift-register outputs, the choice is made using a selection hardware for each transducer. It is important to notice that every output in the shift-register is in fact a sigma-delta modulated signal that can be used to reconstruct the original signal.

The selection is made using a 512 to 1 multiplexer (MUX) for each output transducer. The multiplexer inputs are directly connected to the SR outputs and the selection of each output is made through the select input of each MUX (figure 5.11). The select input of the multiplexers (SELECT VALUE) is a binary value that can be directly extrapolated from the transducer desired delay t_n .

$$\text{SELECT VALUE} = f_{us} \times t_n \quad (5.4)$$

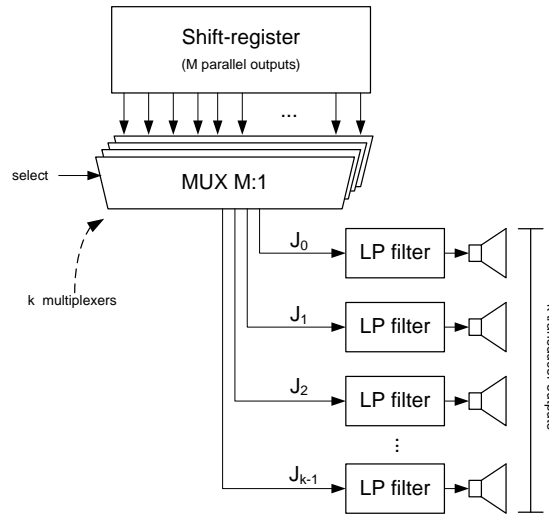


Figure 5.11: Delay selection hardware.

Note that using this multiplexers together with the SR makes the delays update very quickly. Changing the delays takes virtually no time, or more accurately takes one SR clock. This makes the real-time beam-steering possible, depending only the method used to calculate SELECT VALUE. The following section shows the method used to do so, allowing the system to be updated in real time.

5.5.3 Control Unit

The control unit has two distinct functions. The first one is to calculate the necessary delays for each transducer for a certain beam-steering direction and by changing the selected

value to the several multiplexers. The other function is to serve as a communication bridge between the direction angles set by the user and the hardware.

This block can be implemented in a variety of ways either using a software approach, with a micro-controller, or using a hardware approach. In the designed system, the control unit was implemented using the Microblaze processor. The Microblaze is an embedded processor core designed to use with Xilinx FPGAs based on a 32-bit RISC Harvard architecture. Because the Microblaze can be synthesised in the FPGAs, there is no need for additional hardware for this project. Moreover, the designed hardware can be seen as a hardware peripheral to the Microblaze processor, giving the user a more friendly point of view of the system. All the low level control can be made in software without any concern to the hardware itself.

The implemented software does the control of the beam-forming and modulation blocks allowing the emission of a controllable beam of either a simple 40kHz wave or a modulated signal. The delays binary values to input in the multiplexers are calculated accordingly to the equations 3.27 and 5.4.

$$\text{SELECT VALUE}_n = f_{us} \times \left(\frac{x_n \sin(\delta_x)}{V_p} + \frac{y_n \sin(\delta_y)}{V_p} \right) \quad (5.5)$$

To avoid more complex calculations in C using the function *sin*, the computed function is in fact a simplification of the function 5.5 where $\sin(\delta) \approx \delta$ using with δ in radians. This approximation is valid for small angles with an error less than 5% for angles between 0° and 30°. Other way to achieve a more precise *sin* function could be the use of a memory table with the several used angle and respective solutions.

$$\text{SELECT VALUE}_n = f_{us} \times \left(\frac{x_n \delta_x}{V_p} + \frac{y_n \delta_y}{V_p} \right) \quad (5.6)$$

Multiple Beam-formers

Other advantage of using the Microblaze as a hardware controller is the possibility of using a multi-beam-former system. To future applications, the need to have several independent arrays with beam-steering capacity is a probable reality. An example is the use of two parametric arrays in a binaural environment as virtual headphones[18].

To enable the use of two or more independent arrays the control unit can be adapted to control the several connect arrays. The Microblaze can act as a master control (see figure ??) for all the arrays with no need of any extra hardware.

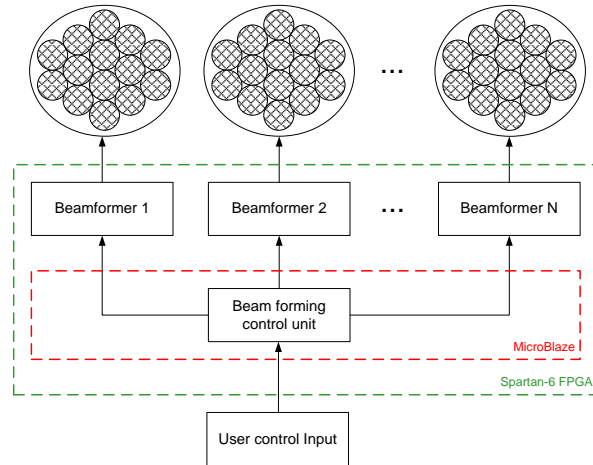


Figure 5.12: Use of multiple beamformers controlled by the same processor.

5.6 Ultrasound transducer array

The ultrasound array was made using MA40S4S Murata piezoelectric transducers disposed in a planar array with a triangular pattern distribution. The signals from the FPGA are amplified using a set of digital buffers and then is filtered with a passive low-pass filter.

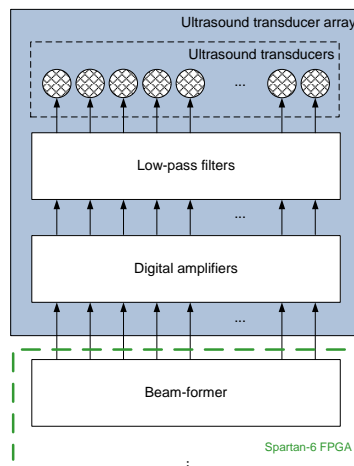


Figure 5.13: Output stage and ultrasound transducer array.

A better description of the amplification and filtering stages are in the following sections.

5.6.1 Amplification digital buffers

The output of the system is in fact a particular case of a class-D amplifier. The sigma-delta modulated signal is a stream of logic '1's and '0's representing respectively high and low voltage. To amplify such a signal only the voltage values between the two logic levels need to be increased, using a digital buffer as amplification stage.

The amplification stage uses in fact a TC4469 integrated chip from Microchip. It is a

logic-input CMOS quad driver with four AND ports with one of the inputs inverted (see logic diagram in figure 5.14).

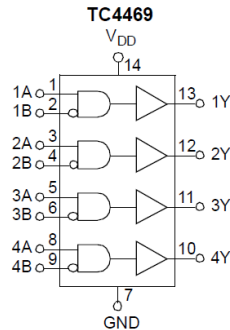


Figure 5.14: TC4469 logic diagram.

The FPGA output was connected to the non-inverted input and the inverted input was connected to the ground (figure 5.15). The supply voltage used to power the TC4469 was it's maximum operating voltage 18V. The output is the original square wave but with low and high values separated by approximately 18V.

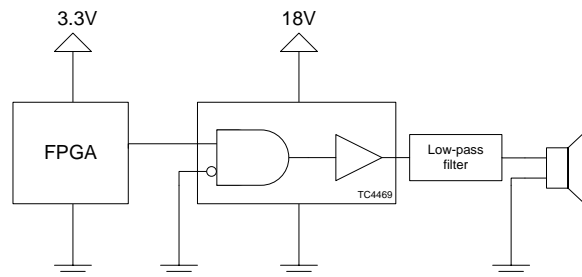


Figure 5.15: Amplification stage

5.6.2 Low pass filters

The output filters' main function is to eliminate the high frequencies replicas of the signal. It is commonly one of the most important parts when using class-D amplifiers, as the overall efficiency reliability and performance depend on it. Although the most common approach is to use a LC filter the projects choice was a low-pass RC filter.

Because the LC uses only reactive components which store the excess energy until it is needed instead of lose some of it into heat, the general efficiency is using higher. However, this particular application has a relatively high number of outputs and therefore the same number of filters. The necessary inductances to construct the filter, are physically too big to make a small device. The first hardware approach used a RC filter with a 3dB cut frequency at 88kHz.

In the section 5.7 some hardware alterations and simplifications that discard the need to use a low pass filter.

5.6.3 Ultrasound transducers

The ultrasound array was made using MA40S4S Murata[19] piezoelectric transducers (figure 5.16). The MA40S4S Murata ultrasound transducers have a nominal frequency of 40kHz and the transducer dimensions are explicit on figure 5.16(d), where it's possible to see that the diameter of each transducer is 9.9mm.

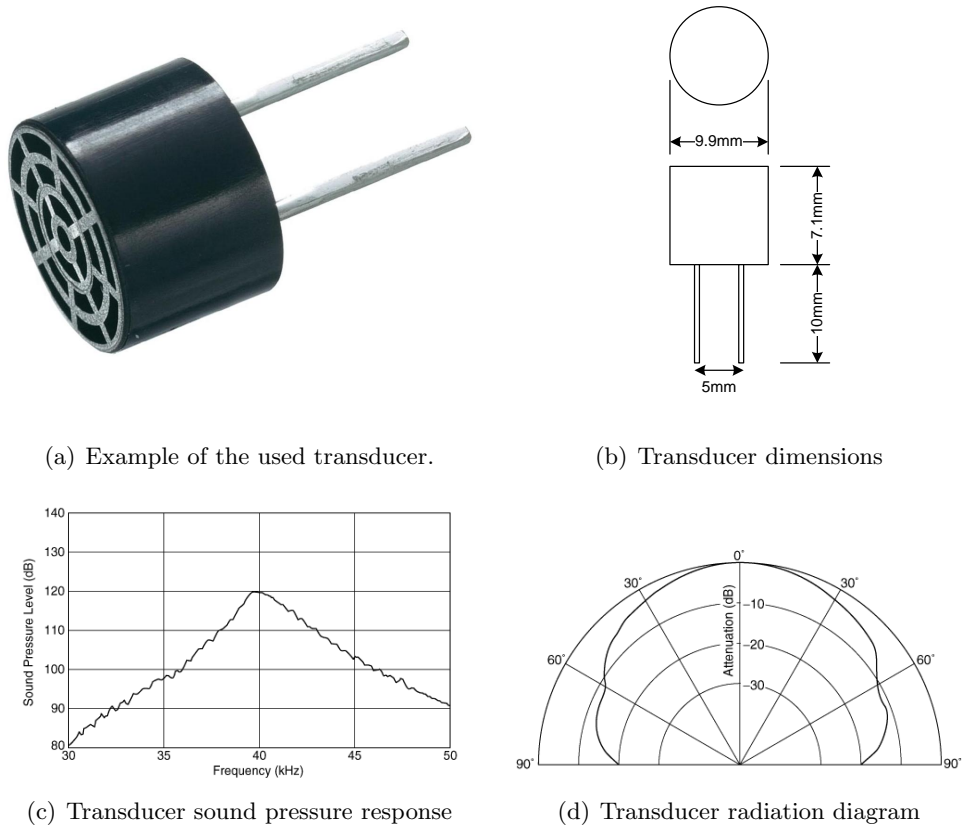


Figure 5.16: MA40S4S Murata piezoelectric transducer.

To use the space as efficiently as possible the array is disposed in triangular pattern accordingly to the one in figure 5.17.

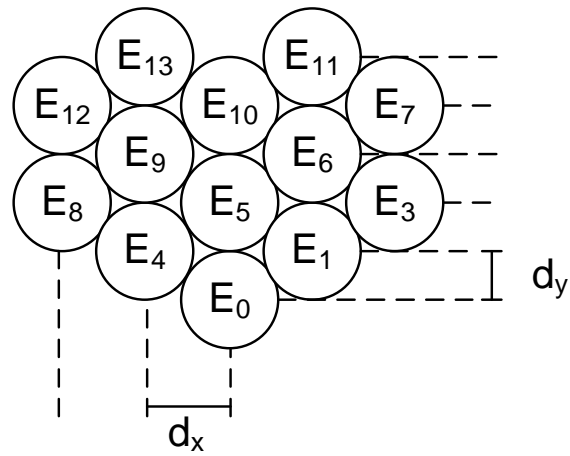


Figure 5.17: Used array pattern.

5.7 Hardware simplifications

The output signal in the modulation block is a 40kHz sinusoidal function with phase modulation accordingly to the sampled signal. Because no amplitude modulation is done, the envelope function is a constant value (see equation 2.6). This means that the shape of the wave, if the envelope is constant, does not have any affect on the air demodulated wave.

Instead of using a regular sine function the system can be simplifying with the use of rectangular have with the same phase as the sine wave. If the instantaneous angular frequency does not change for the rectangular wave, the final demodulated wave is expected to be exactly the same as it would be with a sine wave.

When a SDM input is a square wave at digital full scale the output will be the exact same square wave at output full scale. This means that a square wave modulated using sigma-delta is the exact same square wave at the exact same frequency. In figure 5.18 there's an example showing the difference between the modulation of these two waves.

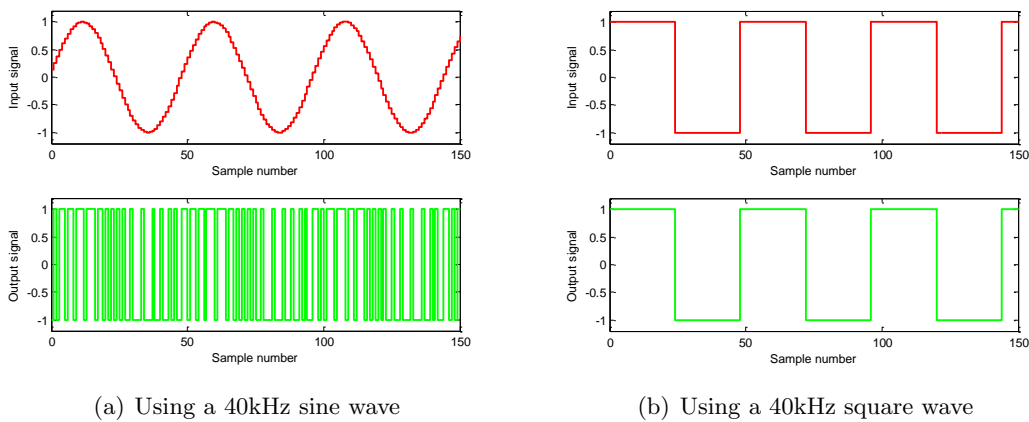


Figure 5.18: Sigma-delta modulator output.

The output wave is a square wave at 40kHz but the phase resolution still is the same because the sigma-delta modulator and shift-register frequency still is 4MHz. The biggest advantage is that now the output wave is in fact a 40kHz square wave instead of 4MHz. The noise electromagnetic interference between signals is now lesser significant than the interference that occurred at 4MHz.

Additionally this leads to some hardware simplifications. Because the square wave is the same in the output as in the input but with a bigger sampling frequency the sigma delta modulator can be simplified to a simple data register. This register is written at the ADC sampling frequency f_s and read at the higher frequency f_{us} .

Other simplification is the elimination of the low-pass filters needed because of the sigma-delta signal. The transducers can be directly driven with a square wave around 40kHz meaning there is no need to use low-pass filter neither to eliminate the 4MHz images nor to smooth the square wave.

It is important to retain that these changes are a particular simplification for the implemented system. These changes are only possible because the demodulating process still occurs when is used a square wave. If the amplitude modulation was used these simplifications couldn't be done because it needs intermediate values for the output voltage instead of only two different values. For other applications that use the same concept to do beam-steering, if a sine wave is necessary, the sigma-delta modulator still is a crucial element to the system.

5.8 Hardware resources

The system simplicity was taken in great consideration in this project. Because it was made to be integrated in other possible projects, the low cost in hardware comes at great importance. To assure that the used hardware stands at low levels, the used FPGA resources were verified. Table 5.1 contains the detailed information of how much FPGA resources were used for every main block in the developed system. The values are considering the use of a 13 emitter ultrasound with the maximum and minimum possible delays as defined in section 5.5.2. The table expresses the quantity of FPGA logic blocks used and the representative percentage relative to the total available blocks. The term LUT stands for Look-up Table and the term BRAM stands for block RAM (each block RAM is 18Kb in size).

Hardware block	Flip-Flops		LUTs		BRAMs	
	quantity	% used	quantity	% used	quantity	% used
ADC controller	17	0.0%	9	0.0%	0	0.0%
PM modulator	115	0.1%	80	0.1%	8	3.0%
Beamformer(total)	531	0.3%	2246	2.4%	0	0.0%
SDM	19	0.1%	36	0.0%	0	0.0%
Shift-register	512	0.3%	0	0.0%	0	0.0%
Multiplexers	0	0.0%	2210	2.4%	0	0.0%
MicroBlaze	2720	1.5%	3197	3.5%	32	11.9%
Total	3383	1.9%	5532	6.0%	40	14.9%

Table 5.1: FPGA resources used.

It is possible to see that the whole system uses a small fraction of the available resources. Furthermore the majority of those resources are in fact spent in the MicroBlaze processor. The

resources used in the processor are in fact not only the from core processor, but also includes the necessary logic for all the peripherals to communicate with the processor, including the connecting logic between the processor and the project implemented hardware.

This processor is in fact an auxiliary support to help functioning with implemented hardware in a more friendly way, and can be either diminished in terms of hardware resources or even replaced by a simpler system. This makes even more noticeable the low hardware requirements needed to implement such a system.

5.9 Prototypes

Most of the designed hardware was made in the FPGA, however the ultrasound transducer array block described in section 5.6 was implemented with additional hardware. Two prototypes were created, the first one, made during the project development, was made using discrete DIP components in a breadboard (see figure 5.19). Not necessary the best option when using sigma-delta signals with 4MHz, it was a very practical approach to test some hardware simplifications already described, that lead to a more compact and efficient final implementation.

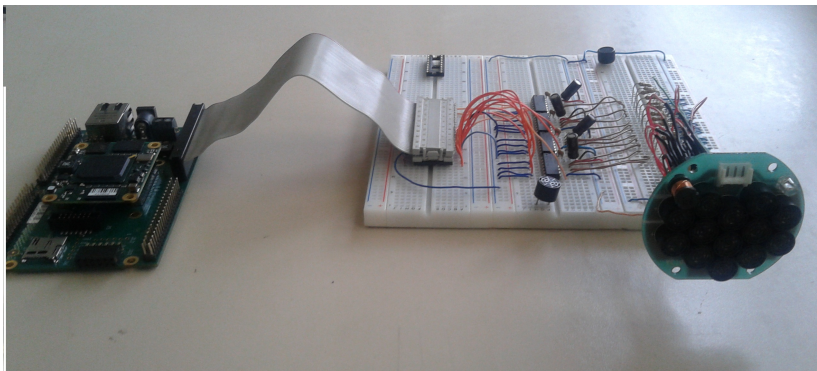
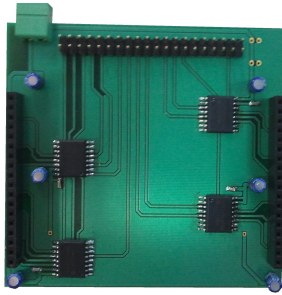


Figure 5.19: Breadboard prototype.

The second prototype (see figure 5.20) was made to achieve a small compact module with purpose of future use in other projects. Design in a PCB it has a total of 28 ultrasound transducers giving it a better directivity and wave gain which translates in a louder volume to the audible sound. The circuit layout can be found in the appendix B.

Both prototypes can interact with user through the Microblaze. Because system was implemented in the GigaBee XC6SLX it allows a variety of possibilities to communicate with the user. Ethernet and a simple UART were the considered protocols to communicate with the device. Ethernet seemed a good choice considering not only its speed but also because it would enable to insert such modules in a network. It could even allow the data streaming of the audible signal making the ADC not necessary. If the device is to be in some kind of network in a future application it is not negligible the possibility of Ethernet communication. Nonetheless, Ethernet is a relatively complex protocol to implement and it would escape from the project purpose.

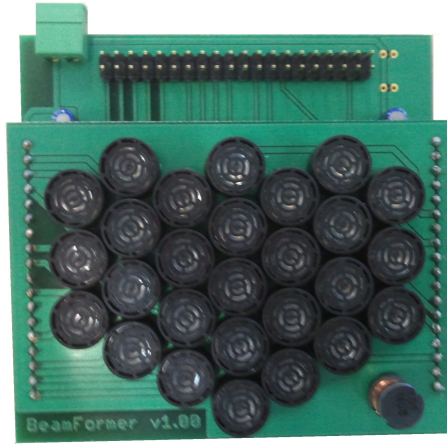
The final choice was the use of a UART which receives commands from the user. A set of commands were defined with tough in a real time beam-steering but also considering the system test. The user has the options of start or stop the signal emission, start or stop the



(a) Bottom PCB.



(b) Top PCB.



(c) Both PCB mounted together.

Figure 5.20: PCB beamformer prototype.

modulation, send 5ms pulses and steering the main lobe to every direction in front of the array in a -25° to 25° cone in a 1° grid.

Chapter 6

Results

6.1 Introduction

The main objective is to prove that the system as described in chapter 5, is able to fulfil the presented objectives. With the objective of observing if a precise beam-steering is achieved an experiment capable of observing the space acoustic pressure was made.

The sound pressure measures were taken using a microphone on top of a XY table moving platform. The XY table allows its platform to move horizontally along x and y axis with a precision that can achieve the 1/1000th of a millimetre.

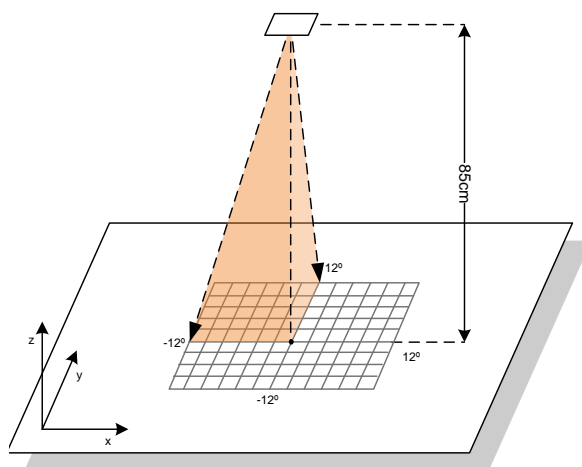


Figure 6.1: Measuring scheme using a x-y table.

The experience display set is shown in figure 6.1. It used the beam-forming system mounted in a distance of 85cm above the microphone (considering the origin position $(0^\circ, 0^\circ)$). The system was set to send a 5ms pulse when a control command was send. For each position in the XY table the pulse would be recorded with a sampling frequency of 96kHz and its FFT would be analysed. The realised FFT used a total of 384 samples considering only samples were the pulse is being received, meaning that 4ms ($384\text{samples}/96000\text{Hz}$) are in fact analysed (see figure 6.2). From the FFT only the 40kHz bin was considered so that external source sounds don't compromise the measures taken.

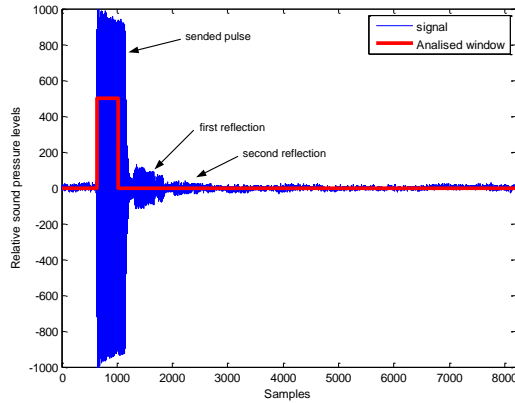


Figure 6.2: Analysed 40kHz pulse.

6.2 Centered beam

The first experience was to observe the beam-forming with no steering angle, this is no delays implemented by the system. The measures were taken in a x-y grid covering up to 12 degrees in each direction either in the x axis as in y axis creating a 12 degrees by 12 degrees square with the measures taken with a 0.5 degrees step.

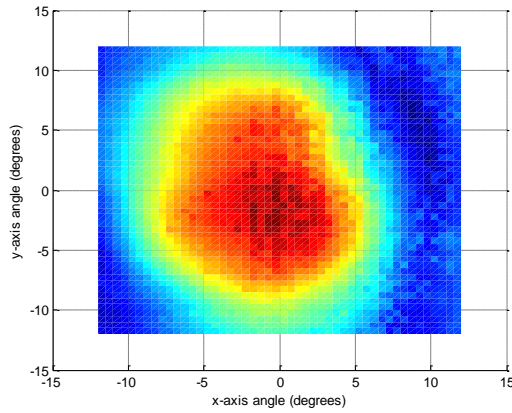


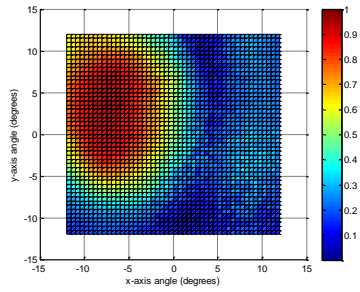
Figure 6.3: Beam direction $(0^\circ, 0^\circ)$.

6.3 Correct position beam-steering test

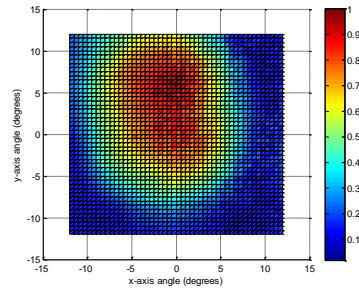
The measures were done to a set of steering angles and then compared to the initial no steering case. The results are in figure 6.5.

Test	Pretended angle (δ_x, δ_y)	Measured angle (δ_x, δ_y)	Directivity
a)	$(-5^\circ, 5^\circ)$	$(-7^\circ, 3^\circ)$	5.4499 dBi
b)	$(0^\circ, 5^\circ)$	$(0^\circ, 5^\circ)$	5.1415 dBi
c)	$(5^\circ, 5^\circ)$	$(4^\circ, 5^\circ)$	4.9783 dBi
d)	$(-5^\circ, 0^\circ)$	$(-7^\circ, 2^\circ)$	6.0432 dBi
e)	$(5^\circ, 0^\circ)$	$(4.5^\circ, 1.5^\circ)$	5.5276 dBi
f)	$(-5^\circ, -5^\circ)$	$(-7^\circ, -5^\circ)$	6.4323 dBi
g)	$(0^\circ, -5^\circ)$	$(0^\circ, -5^\circ)$	5.4144 dBi
h)	$(5^\circ, -5^\circ)$	$(4.5^\circ, -4.5^\circ)$	6.0288 dBi

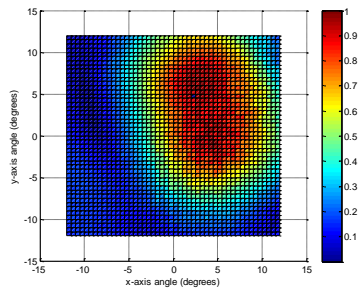
Table 6.1: Main lobe position test



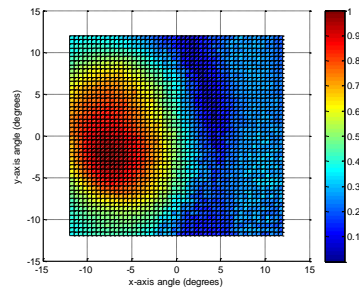
(a) Beam direction $(-5^\circ, 5^\circ)$



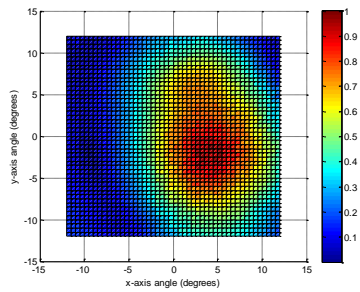
(b) Beam direction $(0^\circ, 5^\circ)$



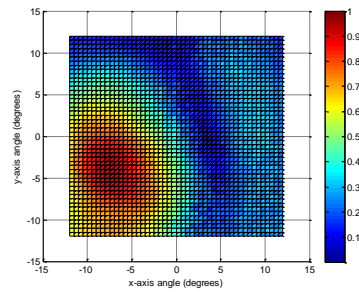
(c) Beam direction $(5^\circ, 5^\circ)$



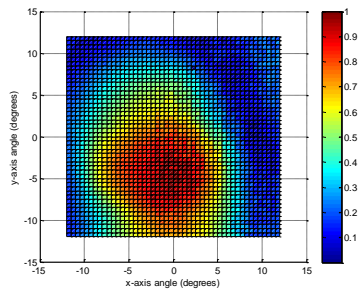
(d) Beam direction $(-5^\circ, 0^\circ)$



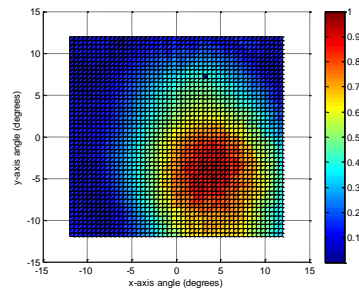
(e) Beam direction $(5^\circ, 0^\circ)$



(f) Beam direction $(-5^\circ, -5^\circ)$



(g) Beam direction $(0^\circ, -5^\circ)$



(h) Beam direction $(5^\circ, -5^\circ)$

Figure 6.4: Acoustic pressure results using beam-steering

6.4 Angle resolution test

Similar to the previous experiment and using the same measurement conditions, this test have the purpose to see if the smallest steering angle and consequent angle resolution are in fact the predicted. Remembering that the smallest steering angle was defined to be between 1° and 2° .

To verify the angle resolution, a steer along the x -axis was made between -5° and 5° spaced between them by 1° .

Test	Pretended angle	Measured angle	Directivity
a)	-5°	-6°	5.6521 dBi
b)	-4°	-5°	5.4399 dBi
c)	-3°	-4°	5.3492 dBi
d)	-2°	-2.5°	5.2360 dBi
e)	-1°	-1°	5.4255 dBi
f)	-0°	0°	5.8637 dBi
g)	1°	1.5°	5.8374 dBi
h)	2°	2.5°	5.6784 dBi
i)	3°	3.5°	5.5922 dBi
j)	4°	4.5°	5.5754 dBi
k)	5°	6°	5.7561 dBi

Table 6.2: Angle resolution test.

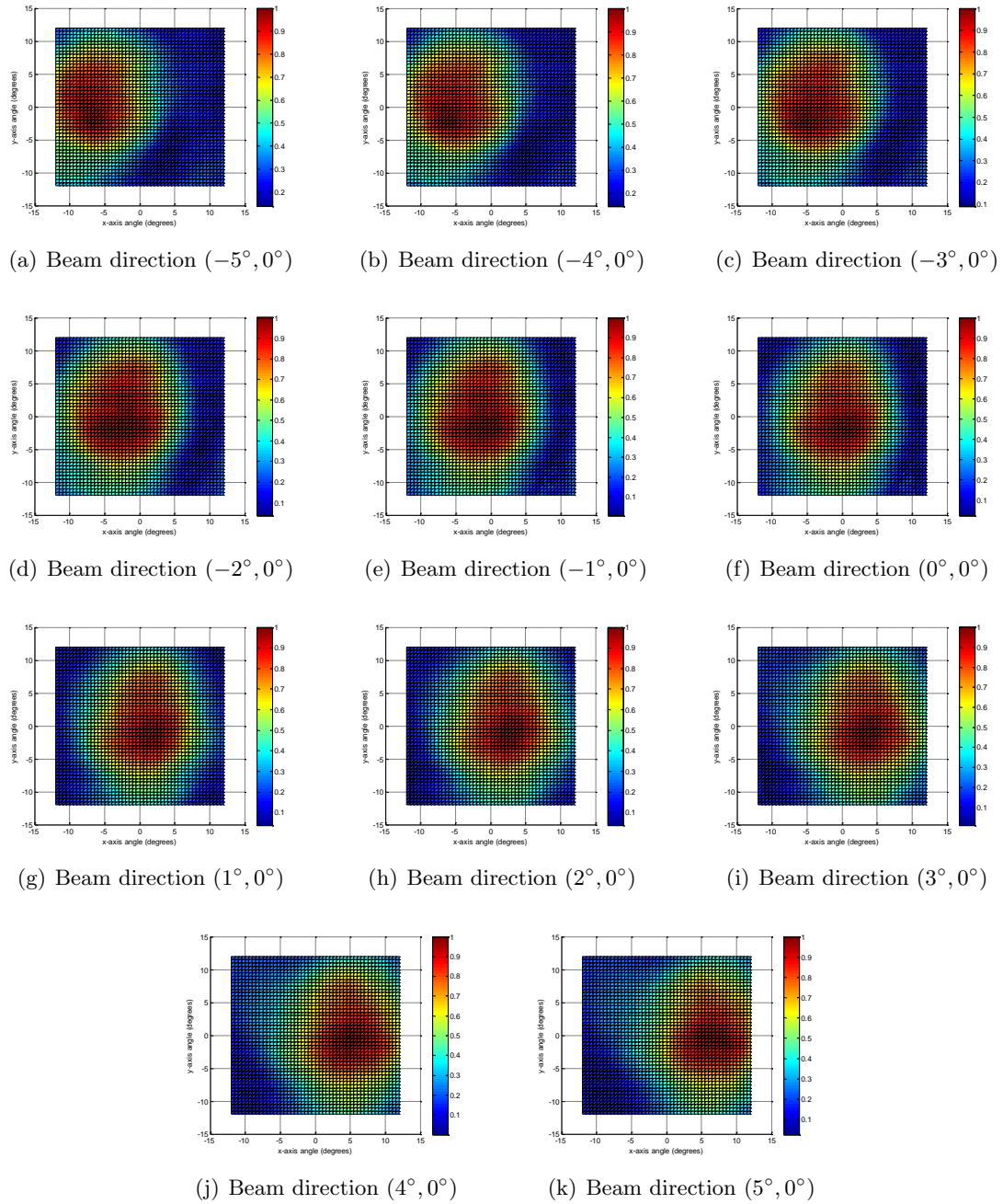


Figure 6.5: Acoustic pressure results using beam-steering

6.5 Results commentaries

With a global analysis the results are the expected for such a system. The power beam is in deed focused towards the desired directions without any significant loss of the beam integrity. The first test had the objective to check if the relative positioning of the sound pressure beam was controlled accordingly the user inputs.

Despite successfully steering the main lobe, some deviations to the pretended positioning

were detected. This deviations go up to 2 degrees, which is reasonable in a system that sets the goal for an angle resolution between 1 and 2 degrees. Plus, this deviation can also be partially caused by the testing set. To maintain the ultrasound array above the XY table, it was suspended using a group of cables. This caused two problems that could translate in small errors in measures. Because the array was suspended by wires, small oscillations could occur which could deviate the array from its initial position. Additionally, and probably a more problematic factor, the array surface could have been in a position that wasn't exactly parallel to the XY table, making small errors in the measures obtained.

The second test had the objective of showing that in fact the resolution stipulated was achieved. Looking at the results is possible to see that in fact, the system can be steered to two different angles less than 2 degrees apart from each other without any degradation of the main power lobe. The graphics show clearly the lobe moving from the left to right always maintaining the same pattern at different angle position separated by less than 2 degrees.

Chapter 7

Conclusions and future work

7.1 Conclusions

For a general point of view the main objectives of this system were accomplished assuming that the proposed hardware implementation fulfil all the requirements. From the tests made using the XY table it was possible to get an area representation of the sound pressure in the surface in front of the emitting array. The beam-steering was measured and analysed for several steering directions varying in the planes z-y and x-y. The results demonstrate a resolution angle, between 1° and 2° , similar to the one expected through simulations.

The first test shows that it is possible to realize the beam-steering of the signal through the desired direction in a very directional and focused way. Even with small angle errors, the system shows a better precision comparing with many of the available solutions of today, maintaining the main lobe integrity and its directivity. It is also important to note, that there are no perceptible degradation of the sound quality when the steering is done. Most impressive than that, is the system's smallest steering angle. In the angle resolution test, the angle sweep shows that in fact the proposed resolution is achieved with a smallest steering angle between 1° and 2° . Joining this high resolution with the real-time beam-steering capacity, this project has achieved its main goals.

Not being the main objective to this project, the analysis of the air demodulated signal quality was made. From all the modulations tested using amplitude modulation or phase/frequency modulation, the one that revealed better quality, this is a better perceptible relation between signal and noise levels, was the phase modulation. Because of the previous use of the DDS as a sinusoidal 40kHz wave generator, the modulation implementation was also much simpler to implement when comparing to amplitude modulations, leading to no increase in the system complexity.

When comparing to other systems with the same objectives, this system has the following advantages:

- Higher angular resolution steering when comparing to similar systems and possibility to increase even further that resolution.
- Provides a real-time beam-steering with almost no processing needs.
- The system was simplified in hardware resources to a very simple system facilitating a cheaper hardware implementation.

- The taken approach doesn't use DAC for every transducer and is more resource efficient especially when using an ultrasound array with many transducers.
- Energy efficient signal amplification using a commutated class D amplifier through a sigma-delta signal.
- The use of a 1-bit delay network replaces the necessity of a more complex delay method and therefore uses less hardware resources.

7.2 Future work

The future work in this project can be divided into two distinct cases. First of all, the continuity of this project to improve the system functionality and quality. The main improvement in terms of functionality is to do the control of two or more ultrasound arrays at the same time. The possibility for a multiple beam-former was considered and the system was made to allow such, however it wasn't implemented or tested because of its deviation from the project objectives.

Other improvement possible is the enhancement of the demodulated audible sound. Even though several signal modulations were tested and the most pleasant to the human ear was chosen, some better techniques can be applied. The modulation used can be changed or be complemented with additional pre-processing and pre-distortion techniques to allow a better demodulation gain and signal quality.

Other possible future work area is the use of such a system in other related projects, or projects that can use it as a peripheral component. The binaural audio device known as virtual headphones is an example of a project that can take advantage of a system with this angle resolution and dimensions.

Appendix A

High order sigma-delta

A.1 Introduction

This chapter consists in the study and project of a VHDL library for the synthesis and implementation of a parameterizable sigma-delta DAC concerning the numbers of entry bits, order and bandpass. This implementation was made using FPGA Spartan-6 by Xilinx on a Atlys Spartan-6 FPGA Development Board. The structure of choice was based on a cascade integrators feedback form, also known as CIFB, and the segmentation of elementary blocks that can be reused accordingly to the desired sigma-delta modulator order. The Implementation done can be exported to any Spartan-6 FPGA.

The use of sigma-delta DAC is usually a compact approach in many digital circuits, being commonly used as because of its low need for additional hardware. It is often used in audio applications, especially portable ones, for allowing a class D amplification known by its power efficiency.

The use of high order sigma-deltas allows a better signal quality by filtering the noise with a superior order filter. In fact the noise transfer function (NTF), is a high pass filter to the noise that attenuates it for the band-pass of the signal.

There are a several ways of implementing higher order SDM, however the four canonical structures are the most common. They are the integrator cascade, in feedback or feedforward, and the cascade resonator in feedback or feedforward. For further details about the canonical structures see [20].

A.2 Implemented structure

For simplicity reasons and similarity to the first-order SDM, the implemented structure was the cascade integrator in feedback (CIFB) shown in A.1.

With this structure as a base point, a set of simpler structures were created. Three distinct types of hardware blocks were created.

First Block Initial block responsible for the bit expansion necessary to the internal functionality

Basic Block Most basic block responsible for the multiplication and integration operations.

Last Block The final block which quantizes the resulting signal from the previous blocks and sends the feedback signal. It also responsible for the 1-bit out put.

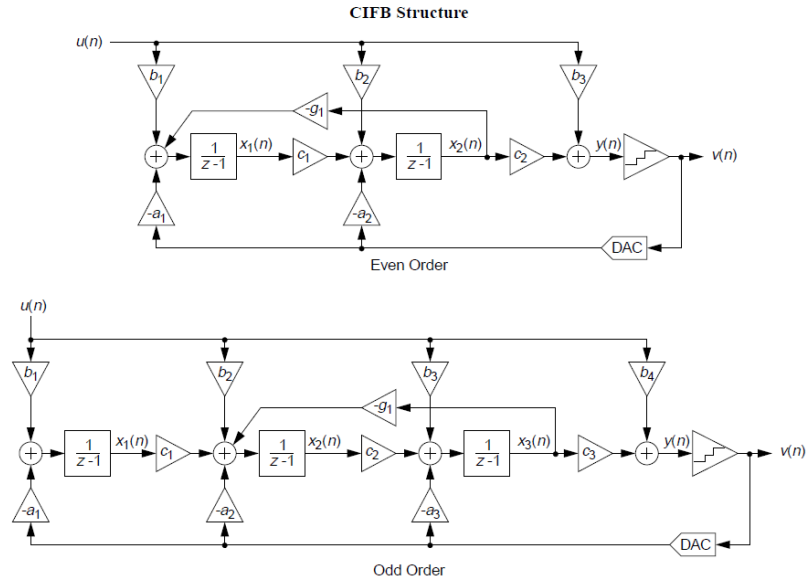


Figure A.1: Cascade integrator feedback structure.

These blocks are connected to each other as explicit in figure A.2.

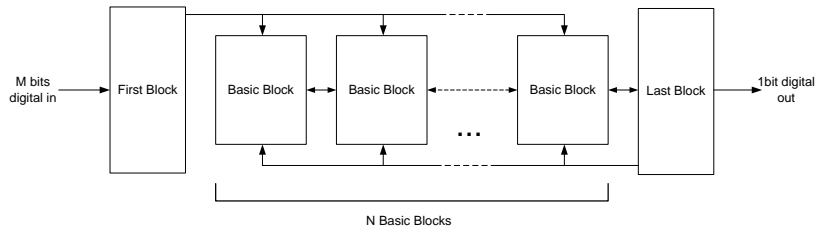


Figure A.2: N-th order sigma-delta modulator.

The one or more basic blocks are in fact what defines the order and bandpass of the SDM. The order is directly connected to the number of basic blocks used connected in a cascade between them. The band-pass is configured by defining the internal multipliers constants a_i , b_i , c_i and g_i . These constants are constant for each SDM, and are defined in synthesis time, not being changeable once the hardware is synthesise.

The figure A.3 shows the basic block internal structure which is accordingly to the CIFB structure shown before.

For the correct behaviour of the SDM it is necessary to apply the correct values for the coefficients a , b , c and g . These values are obtained trough the desired noise transfer function (NTF) and signal transfer function (STF). Because it is a relative complex analysis and algorithm to implement the values were obtain using a MATLAB Toolbox. The Delta Sigma Toolbox by Analog Devices[21] uses the oversampling ratio value, the desired bandwidth, the desired order and the structure to calculated the STF and NTF and consequently the values of a_i , b_i , c_i and g_i to be used as parameters in the VHDL synthesiser.

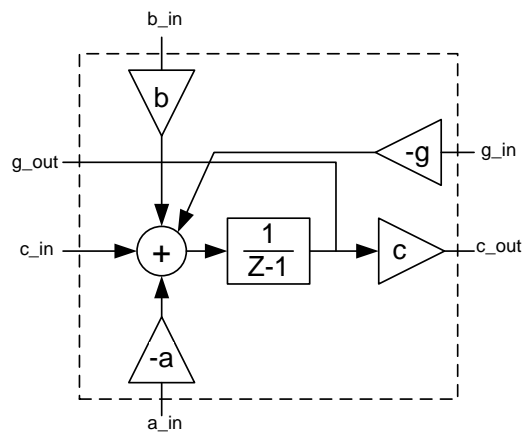


Figure A.3: Basic block internal structure.

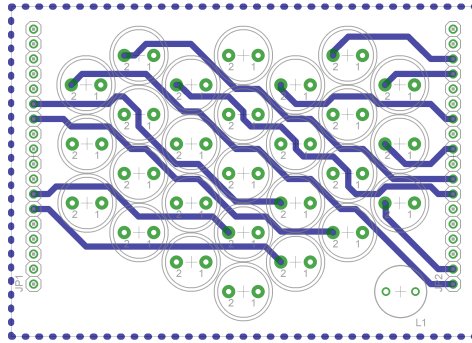


Figure B.3: Bottom view of the ultrasound array of beamformer board.

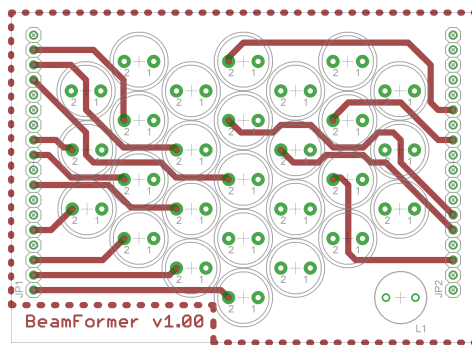


Figure B.4: Top view of the ultrasound array part of beamformer board.

Bibliography

- [1] Nicera. Parametric speaker, April 2012.
- [2] Holosonics. Audiospotlight, March 2012.
- [3] Sennheiser. Audiobeam, March 2012.
- [4] Woon-Seng Gan, Jun Yang 0004, K.-S. Tan, and Meng Hwa Er. A digital beamsteerer for difference frequency in a parametric array. *IEEE Transactions on Audio, Speech and Language Processing*, 14(3):1018–1025, 2006.
- [5] D. I. Havelock and A. J. Brammer. Directional loudspeakers using sound beams. *Journal of the Audio Engineering Society*, 48(10):908 –916, 2000.
- [6] F. Joseph Pompei. *Sound From Ultrasound: The Parametric Array as an Audible Sound Source*. PhD thesis, Massachusetts Institute of Technology.
- [7] Peter J Westervelt. Parametric acoustic array. *Journal of the Acoustical Society of America*, 35(4):535–537, 1963.
- [8] H.O. Berktaay. Possible exploitation of non-linear acoustics in underwater transmitting applications. *Journal of Sound and Vibration*, 2(4):435 – 461, 1965.
- [9] M B Bennett and D T Blackstock. Parametric array in air. *Journal of the Acoustical Society of America*, 57(3):562–568, 1975.
- [10] Ee-Leng Tan, Peifeng Ji, and Woon-Seng Gan. On preprocessing techniques for bandlimited parametric loudspeakers. *Applied Acoustics*, 71(5):486 – 492, 2010.
- [11] Ronald N. Bracewell. *The Fourier transform and its applications / Ronald N. Bracewell*. McGraw-Hill, New York :, 2d ed. edition, 1978.
- [12] B.D. Van Veen and K.M. Buckley. Beamforming: a versatile approach to spatial filtering. *ASSP Magazine, IEEE*, 5(2):4 –24, april 1988.
- [13] Toby Haynes. A Primer on Digital Beamforming, March 1998.
- [14] Digital Converters. *Management*, 1999.
- [15] Digilent. *Digilent PmodAD Analog To Digital Module Converter Board Reference Manual*.
- [16] Analog Devices. *AD7476A Data sheet*.

- [17] Xilinx. *LogiCORE IP DDS Compiler v4.0*.
- [18] Daniel Menzel, Helmut Wittek, Gunther Theile, Hugo Fastl, Ag Technische Akustik, and Technische Universitat Munchen. The binaural sky: A virtual headphone for binaural room synthesis. In *In International Tonmeister Symposium Schloss Hohenkammer*, 2005.
- [19] Murata. *Murata MA40S4S Data sheet*.
- [20] Gabor C. Temes Richard Schreier. *Understanding Delta-Sigma Data converters*. Wiley-IEEE Press, Novembro 2004.
- [21] Richard Schreier. *THE DELTA-SIGMA TOOLBOX Version 7.3 Manual*. Analog Devices, Inc., Julho 2009.
- [22] A.J. Magrath, I.G. Clark, and M.B. Sandler. Design and implementation of a fpga sigma-delta power dac. In *Signal Processing Systems, 1997. SIPS 97 - Design and Implementation., 1997 IEEE Workshop on*, pages 511 –521, nov 1997.
- [23] F. Joseph Pompei. The use of airborne ultrasonics for generating audible sound beams. In *Audio Engineering Society Convention 105*, 9 1998.
- [24] Peifeng Ji, Chao Ye, and Jing Tian. Development of a directional loudspeaker system for sound reproduction. In *Multimedia and Expo, 2007 IEEE International Conference on*, pages 591 –594, july 2007.
- [25] B.D. Steinberg. Digital beamforming in ultrasound. *Ultrasonics, Ferroelectrics and Frequency Control, IEEE Transactions on*, 39(6):716 –721, nov. 1992.
- [26] Prabhakar S. Naidu. *Sensor Array Signal Processing*. CRC Press, Inc., Boca Raton, FL, USA, 2000.
- [27] Don H. Johnson and Dan E. Dudgeon. *Array signal processing : concepts and techniques / Don H. Johnson, Dan E. Dudgeon*. P T R Prentice Hall, Englewood Cliffs, NJ :, 1993.